

University of Warwick institutional repository: <http://go.warwick.ac.uk/wrap>

This paper is made available online in accordance with publisher policies. Please scroll down to view the document itself. Please refer to the repository record for this item and our policy information available from the repository home page for further information.

To see the final version of this paper please visit the publisher's website. Access to the published version may require a subscription.

Author(s): Z. Tamainot-Telto, S.J. Metcalf, R.E. Critoph, Y. Zhong, R. Thorpe

Article Title: Carbon–ammonia pairs for adsorption refrigeration applications: ice making, air conditioning and heat pumping

Year of publication: 2009

Link to published article:

<http://dx.doi.org/10.1016/j.ijrefrig.2009.01.008>

Publisher statement: "NOTICE: this is the author's version of a work that was accepted for publication in International Journal of Refrigeration. Changes resulting from the publishing process, such as peer review, editing, corrections, structural formatting, and other quality control mechanisms may not be reflected in this document. Changes may have been made to this work since it was submitted for publication. A definitive version was subsequently published in International Journal of Refrigeration, [VOL:32, ISSUE:6, September 2009, DOI: 10.1016/j.ijrefrig.2009.01.008,"

Carbon-Ammonia pairs for adsorption refrigeration applications: ice making, air conditioning and heat pumping

Z. Tamainot-Telto⁽¹⁾, S.J. Metcalf, R.E. Critoph, Y. Zhong., R. Thorpe
School of Engineering - University of Warwick
Coventry CV4 7AL – United Kingdom (UK)

Abstract – A thermodynamic cycle model is used to select an optimum adsorbent-refrigerant pair in respect of a chosen figure of merit that could be the cooling production (MJ m^{-3}), the heating production (MJ m^{-3}) or the coefficient of performance (COP). This model is based mainly on the adsorption equilibrium equations of the adsorbent-refrigerant pair and heat flows. The simulation results of 26 various activated carbon-ammonia pairs for three cycles (single bed, two-bed and infinite number of beds) are presented at typical conditions for ice making, air conditioning and heat pumping applications. The driving temperature varies from 80°C to 200°C . The carbon adsorbents investigated are mainly coconut shell and coal based types in multiple forms: monolithic, granular, compacted granular, fibre, compacted fibre, cloth, compacted cloth and powder. Considering a two-bed cycle, the best thermal performances based on power density are obtained with the monolithic carbon KOH-AC with a driving temperature of 100°C , the cooling production is about 66 MJ m^{-3} (COP=0.45) and 151 MJ m^{-3} (COP=0.61) for ice making and air conditioning respectively; the heating production is about 236 MJ m^{-3} (COP=1.50).

(Keywords: Adsorption, Air conditioning, Ammonia, Carbon, Heat pump, Ice making, Refrigeration)

Les paires charbon actif-ammoniac pour les applications de réfrigération à adsorption: fabrication de la glace, climatisation et pompe à chaleur

Un modèle du cycle thermodynamique est utilisé pour sélectionner le meilleur couple adsorbant-ammoniac sur la base de la production frigorifique (MJ m^{-3}), la production de chaleur (MJ m^{-3}) ou bien le coefficient de performance (COP). Ce modèle est essentiellement basé sur les équations d'état de l'adsorption (adsorbant-ammoniac). Les résultats de simulation de 26 différentes paires charbon actif-ammoniac sont présentés pour des conditions typiques de fabrication de la glace, de climatisation et de pompe à chaleur. La température de génération varie de 80°C à 200°C . Les simulations sont effectuées pour trois types de cycle: lit unique, deux-lits et un nombre infini de lits. Les charbons actifs étudiés sont essentiellement issus des coquilles de noix de coco et de minerais de charbon sous diverses formes: monolithique, granulaire, granulaire compacté, fibre, fibre compactée, tissu, tissu compacté et poudre. En considérant un cycle à deux lits, les meilleures performances thermiques sont obtenues avec le charbon monolithique KOH-AC: avec une température de génération de 100°C : la production frigorifique est environ 66 MJ m^{-3} (COP=0.45) et 151 MJ m^{-3} (COP=0.61) pour la fabrication de la glace et la climatisation respectivement; la production de chaleur est environ 236 MJ m^{-3} (COP=1.50).

(Mots clés: Adsorption, Conditionnement d'air, Ammoniac, Charbon, Pompe à chaleur, Machine à glace, Réfrigération)

⁽¹⁾ Corresponding author: E-mail es2071@eng.warwick.ac.uk - Tel. +44 24 76522108 – Fax +44 24 76418922

NOMENCLATURE

<i>A</i>	Ammonia characteristic coefficient (K)
<i>C</i>	Specific heat ($\text{J kg}^{-1} \text{K}^{-1}$)
<i>COP</i>	Coefficient of performance
<i>h</i>	Specific enthalpy (J kg^{-1})
<i>H</i>	Specific heat of sorption (J kg^{-1})
<i>k</i>	Dubinin coefficient
<i>n</i>	Dubinin coefficient
<i>q</i>	Heat density (J m^{-3})
<i>Q</i>	Heat (J kg^{-1})
<i>P</i>	Pressure (Pas or Bar)
<i>R</i>	Ammonia gas constant ($\text{J kg}^{-1} \text{K}^{-1}$)
<i>SEE</i>	Standard Estimated Error
<i>T</i>	Temperature (K or °C)
<i>TR</i>	Tons of refrigeration
<i>x</i>	Concentration ($\text{kg Ammonia kg}^{-1} \text{Carbon}$)

Greek letters

ρ	Density (kg m^{-3})
Δ	Difference, variation

Subscripts

<i>a</i>	adsorbed phase
<i>c</i>	carbon, cooling
<i>C</i>	Condensing, condensation
<i>E</i>	Evaporating, evaporation
<i>G</i>	Generating, generator
<i>H</i>	Heating
<i>In</i>	Input
<i>p</i>	At constant pressure
<i>reg</i>	Regeneration
<i>reject</i>	Rejection, Rejecting

sat Under ammonia saturation conditions

tip Tipping

INTRODUCTION & BACKGROUND

The basic adsorption refrigeration system consists of two linked vessels, one of which contains the adsorbent-refrigerant pair (generator) and the second which contains only refrigerant (evaporator-condenser). Both vessels are initially at low pressure and temperature with a high refrigerant concentration within the adsorbent and only refrigerant gas in the second vessel (**Figure 1**). The first step consists of heating up the generator using the chosen or available heat source: the refrigerant gas is driven out from the adsorbent while the pressure of the full system rises (desorption) (a). The desorbed gas is condensed in the evaporator-condenser by rejecting heat (b). When the generator has reached the minimum or desirable refrigerant concentration (c), it is then cooled to its initial temperature and re-adsorbs the refrigerant, reducing the pressure (adsorption). The lower pressure causes the refrigerant liquid contained in the evaporator-condenser to boil, absorbing heat and therefore producing the necessary cooling effect (d). The basic adsorption refrigeration cycle is intermittent and the cooling production takes place during the half cycle only. However, two or more beds can be operated out of phase to produce continuous cooling. The basic thermodynamic cycle of an adsorption machine is described in **Figure 2**. An adsorption cycle is characterised by four operating temperatures: the generating temperature (T_3), the initial or lower generator temperature (T_1), the condensing temperature (T_C) and the evaporating temperature (T_E).

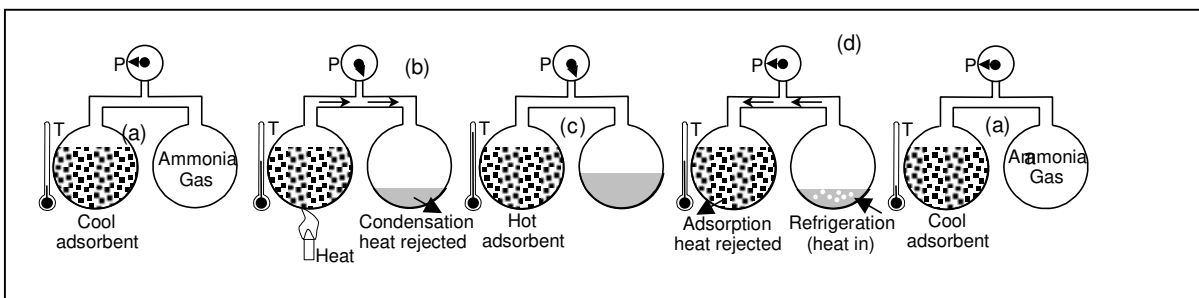


Figure 1: Principle of adsorption refrigeration technology

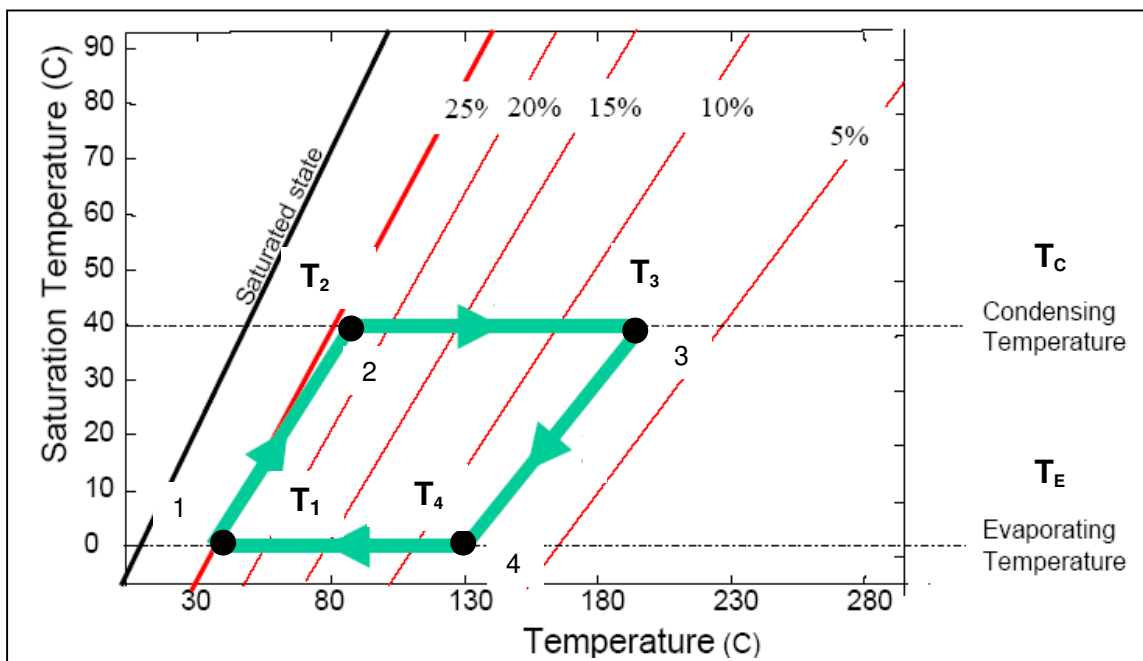


Figure 2: Adsorption thermodynamic cycle

1 to 2 and 2 to 3: Isosteric and isobaric heat input respectively (Desorption process) 3 to 4 and 4 to 1: Isosteric and isobaric cooling (rejected heat) respectively (Adsorption process)

Unlike a conventional refrigeration system driven mechanically by a compressor, the adsorption refrigeration system is a heat driven machine. Since that heat could be widely available or from a waste source, adsorption refrigeration systems offer a great advantage compared with conventional systems. The use of such systems (powered by solar energy or heat generated by burning agricultural waste or biomass in general) in the remote part of developing countries where there is no electricity supply is useful for storage of medical products (vaccine), foods (vegetable, meat, fish, etc.) or habitat comfort (air conditioning). For the food conservation application, the basic adsorption system could provide up to 0.100 TR (equivalent of 100 kg ice/day) with low generating temperature ($100^{\circ}\text{C} < T_3 < 120^{\circ}\text{C}$) [1]. The basic solar sorption technology is not yet as cost effective as the conventional vapour compression cooling system because of its poor specific cooling production: with activated carbon, the typical specific cooling production is less than 20 W kg^{-1} carbon [2-7] corresponding to less than 0.006 TR/kg carbon.

The impact on a vehicle's fuel consumption due to its conventional air conditioning (AC) is a real problem for the automotive industry: about 8% to 15% of car or truck fuel consumption is currently attributed to the AC system [8, 9]. At the same time, a vehicle engine could waste around 60% of the input fuel's energy through the water coolant system and exhaust gas. As the price of fuel increases, it becomes obvious that the development of cost effective (capital and running cost) and environmentally friendly mobile AC is needed. Sorption cooling technology is an attractive alternative, as the system could be powered with waste heat from the engine water cooling jacket (generating temperature up to 100°C) and/or from the exhaust gas (generating temperature up to 200°C); the technology could contribute to substantial fuel savings of up to 20% in a vehicle, therefore reducing gas emissions (CO , CO_2 , NO_x , SO_x ...). In order to make this technology as competitive as conventional mechanical AC technology, it is critical to select an appropriate adsorbent for the generator that leads to high cooling production density and therefore low capital cost.

The space heating during the winter and the hot water requirement throughout the year represents a substantial proportion of energy consumption in the EU: in the UK in 2002, it uses 39% [10]. Therefore improvements in space heating and hot water production efficiency could lead to a significant fuel saving and gas emissions reduction. The gas fired adsorption heat pump is suitable for the replacement of current conventional gas boilers. Once again, the selection of an appropriate carbon-ammonia pair is very important.

This paper presents simulation results for various carbon adsorbents using ammonia refrigerant. The results are then used to identify the adsorbent which gives the highest performance, with the prospect of designing better adsorption refrigeration systems for ice making, air conditioning and heat pumping applications. The thermodynamic model used is mainly based on the adsorption equilibrium equations of the adsorbent-refrigerant pair, the heat required (sensible heat and heat of desorption), the cooling production (latent heat of vaporisation of the refrigerant) and heat production (heat of adsorption and the heat of condensation). The simulation results of various activated carbon-ammonia pairs are investigated at typical conditions: $T_C = 35^{\circ}\text{C}$, $T_E = -5^{\circ}\text{C}$ and $T_1 = 35^{\circ}\text{C}$ for ice making ; $T_C = 35^{\circ}\text{C}$, $T_E = 10^{\circ}\text{C}$ and $T_1 = 35^{\circ}\text{C}$ for air conditioning and $T_C = 40^{\circ}\text{C}$, $T_E = 5^{\circ}\text{C}$ and $T_1 = 40^{\circ}\text{C}$ for heat pumping. The driving temperature T_3 varies from 80°C up to 200°C . Three cycles are investigated: single bed, two-bed and infinite number of beds.

THERMODYNAMIC MODELLING

A program written in Matlab 7.01 is used to estimate of the performance (mainly COP and thermal production) with different cycles (single bed, two-bed with regeneration, and infinite number of beds) at various working conditions. The code is designed to test a large number of pairs providing that the equilibrium equation of the adsorbent-refrigerant pair and the thermophysical properties of both adsorbent and refrigerant are known.

Equilibrium equation

Experimental porosity tests were carried out for each sample and the data fitted to a modified form of the Dubinin-Radushkevich (D-R) equation:

$$x = x_o \exp \left[-k \left(\frac{T}{T_{sat}} - 1 \right)^n \right] \quad (1)$$

where: x is the ammonia concentration (kg ammonia kg⁻¹ carbon); T is the carbon temperature (K); x_o is the ammonia concentration under saturation conditions (kg ammonia kg⁻¹ carbon); T_{sat} is the saturation temperature corresponding to the gas pressure (K).

Heat input (sensible heat and heat of desorption)

The heat input of each bed is calculated by integration of the effective specific heat (dQ/dT) along the process path from the initial temperature T_1 to the generating temperature T_3 as described by Meunier [11]. The specific heat (dQ/dT) along the isosteric path (1-2) is given by:

$$\frac{dQ}{dT} = C_{pc}(T) + xC_{pa} \quad (2)$$

where: C_{pc} is the carbon specific heat (J kg⁻¹K⁻¹) which varies with temperature and C_{pa} is the specific heat of adsorbed phase ($C_{pa} \sim 4900 \text{ J kg}^{-1} \text{ K}^{-1}$ for ammonia).

The specific heat (dQ/dT) along the isobaric path (2-3) is given by:

$$\frac{dQ}{dT} = C_{pc}(T) + xC_{pa} + H \left(\frac{\partial x}{\partial T} \right)_p \quad (3)$$

where: H is the heat of desorption given by the following expression:

$$H = R(P,T) A \frac{T}{T_{sat}} \quad (4)$$

where: R is the gas constant at the system pressure P and temperature T (J kg⁻¹K⁻¹); A is the slope of the saturated adsorbate line on the Clapeyron diagram ($A=2823.4 \text{ K}$); T is the carbon temperature (K); T_{sat} is the saturation temperature corresponding to the gas pressure (K).

Since the ratio T/T_{sat} is constant along an isostere, the temperature at the end of the isosteric pressurisation phase T_2 can be expressed as:

$$T_2 = \frac{T_C}{T_E} T_1 \quad (5)$$

where: T_1 , T_C and T_E are the bed initial, condensing and evaporating temperatures, respectively (K).

Heat rejected (sensible heat and heat of adsorption)

A similar technique is also used to estimate the heat rejected by the bed (heat of adsorption and sensible). All previous equations are unchanged except **equation (3)**, that must take into account the cooling effect on the bed of the cold gas coming from the evaporator, and **equation (5)**. Therefore the specific heat (dQ/dT) along the isobaric path (4-1) is:

$$\frac{dQ}{dT} = C_{pc}(T) + xC_{pa} + [H - (h_{gas}(T) - h_{gas}(T_E))] \left(\frac{\partial x}{\partial T} \right)_p \quad (6)$$

In the same manner as equation (5), the temperature at the end of the isosteric depressurisation stage T_4 may be expressed as:

$$T_4 = \frac{T_E}{T_c} T_3 \quad (7)$$

where: T_3 is the bed temperature at the end of the desorption phase.

The effective specific heat is calculated for every 1 K temperature interval throughout both the heating and cooling processes. The total heat input to the bed Q_{input} corresponds to the sum of the combined sensible heat and heat of desorption and is calculated by integration from equation (2) and equation (3) as illustrated in **Figure 3**.

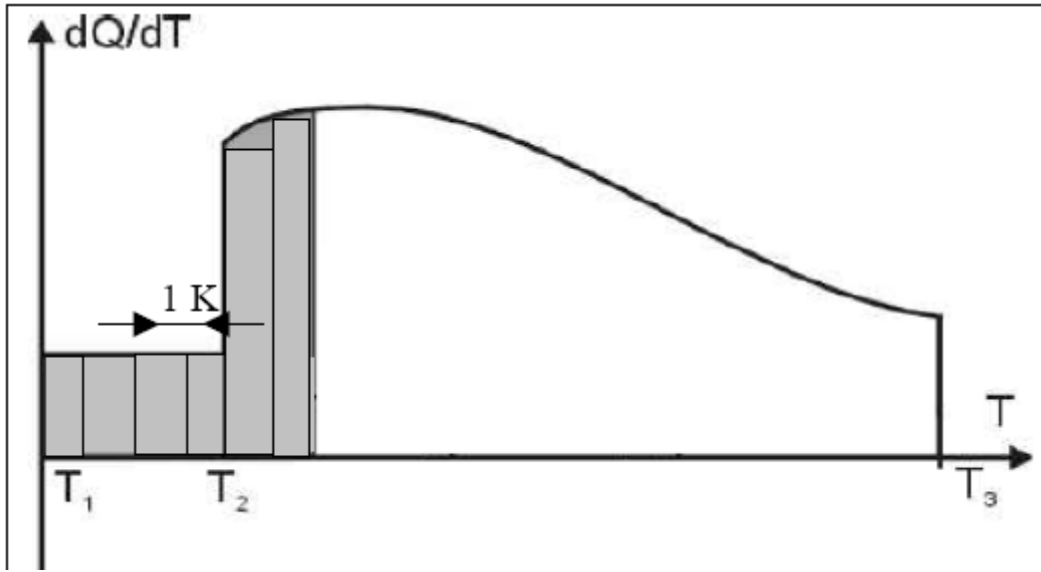


Figure 3: Effective specific heat vs. temperature for a single bed

In the two-bed regenerative cycle as illustrated in **Figure 4**, the heat rejected Q_{reg} from the adsorbing bed between T_3 and T_6 is transferred across a temperature difference and is recovered in order to preheat the desorbing bed from T_1 to T_5 until it reaches a predetermined temperature difference ΔT (typical value 10 K). The total heat input is therefore reduced from $Q_{in} + Q_{reg}$ to Q_{in} and the efficiency of the system is improved.

In the case of an infinite number of beds and ideal heat transfer the maximum amount of rejected heat Q_{reject} is recovered. The total heat input required will be reduced from Q_{in} to $Q_{in} - Q_{reject}$ as illustrated in **Figure 5**, All the methods of heat management in sorption refrigeration systems are well documented [11, 12].

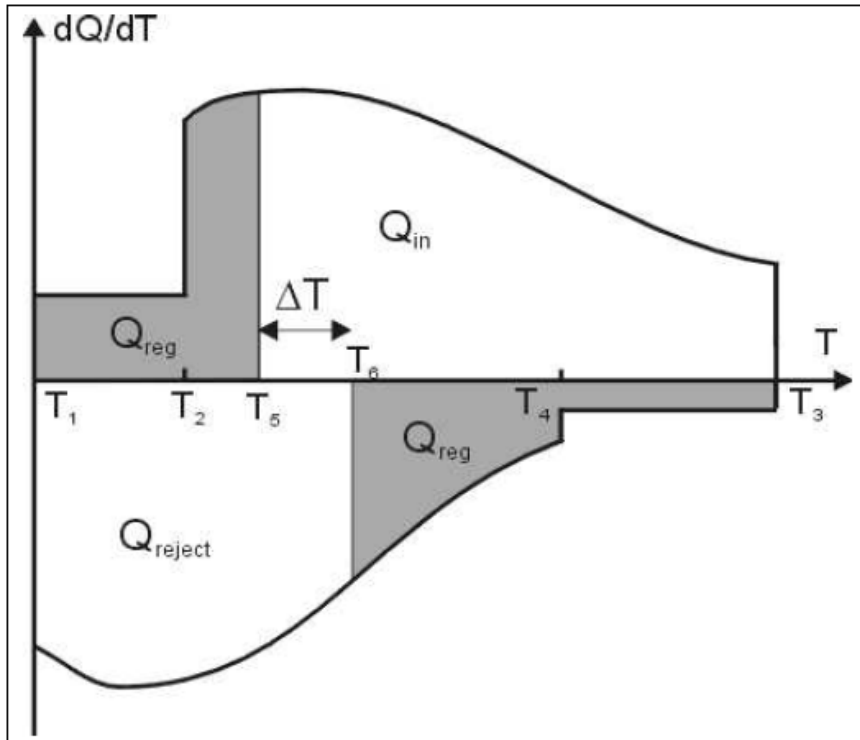


Figure 4: Effective specific heat vs. temperature for a two-bed regenerative cycle [12]

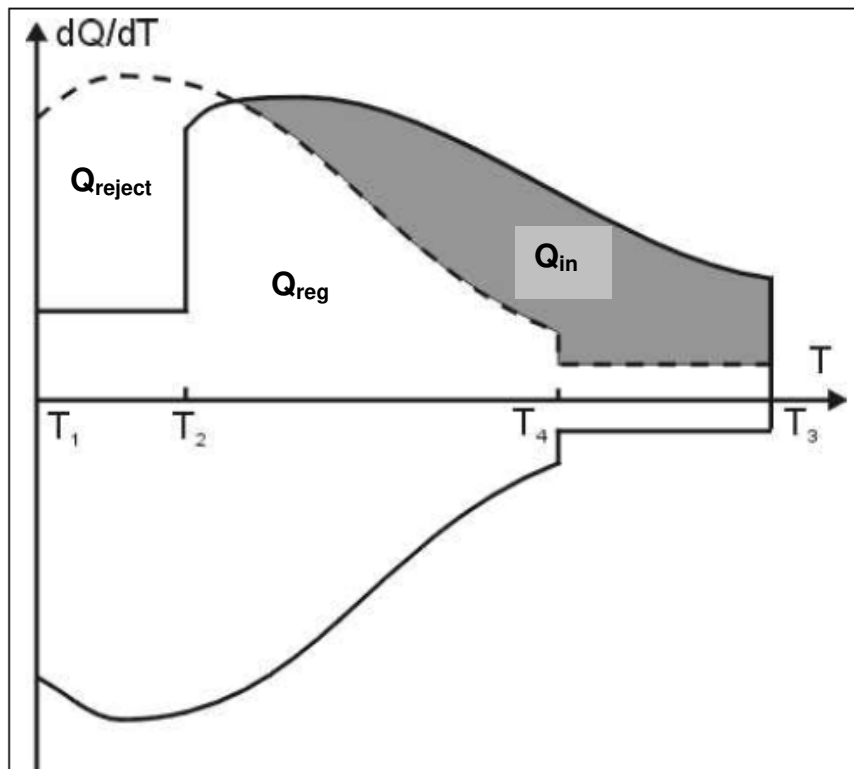


Figure 5: Effective specific vs. temperature in an infinite number of beds [12]

Cooling production and COP_c

The specific cooling production Q_c (kJ kg^{-1} carbon) is characterized by the latent heat of vaporisation of the ammonia liquid collected during the condensation phase:

$$Q_c = \Delta x(h_{gas}(T_E) - h_{liquid}(T_C)) \quad (8)$$

where: Δx is the amount of liquid ammonia collected during the condensation phase ($\text{kg ammonia/kg carbon}$) – corresponding to the net concentration change from the higher isostere line (at T_1) to the lower isostere line (at T_3), and thus the effect of generator void volume is neglected; h_{gas} and h_{liquid} are the specific enthalpies of the gas leaving the evaporator and the condensed liquid (kJ kg^{-1}).

The cooling production could also be expressed per unit volume of carbon q_c (kJ m^{-3}):

$$q_c = \rho Q_c \quad (9)$$

where: ρ is the bulk density of the carbon sample (kg m^{-3})

The cooling coefficient of performance COP_c is the ratio of the cooling production to the heat input:

$$COP_c = \frac{Q_c}{Q_{input}} \quad (10)$$

Heating production and COP_H

From the heat balance throughout the full cycle, the relationship between the cooling coefficient of performance COP_c and the heating coefficient of performance COP_H is given by the following expression:

$$COP_H = COP_c + 1 \quad (11)$$

Since the heating coefficient of performance COP_H is the ratio of the heating production Q_H to the heat input,

$$COP_H = \frac{Q_H}{Q_{input}} \quad (12)$$

The heating production Q_H is therefore given by:

$$Q_H = (COP_c + 1)Q_{input} \quad (13)$$

The heating production could also be expressed per unit volume of carbon q_H (kJ m^{-3}):

$$q_H = \rho Q_H \quad (14)$$

where: ρ is the bulk density of the carbon sample (kg m^{-3})

CARBON-AMMONIA PAIR CHARACTERISTICS

The carbon adsorbents investigated with ammonia refrigerant are mainly coconut shell and coal based types in multiple form: monolithic, granular, compacted granular, fibre, compacted fibre, cloth, compacted cloth and powder. The main properties of each carbon-ammonia pair, namely the Dubinin coefficients (x_0 , K , n) and density (ρ) that were experimentally measured are summarized in **Table 1**.

Reference	Manufacturer	x_0	K	n	SEE	Density (kg m ⁻³)	Carbon Origin
MONOLITHIC CARBON							
LM001	Chemviron Carbon	0.2700	4.3772	1.1965	0.0100	713	Coco Shell
LM127	Chemviron Carbon	0.3629	3.6571	0.94	0.0019	750	Coco Shell
LM128	Chemviron Carbon	0.3333	3.6962	0.99	0.0028	715	Coco Shell
LM279	Chemviron Carbon	0.3837	4.2434	1	0.0030	840	Coco Shell
SDS	ATMI	0.2450	5.6069	2.1389	0.0093	1120	PVDC
KOH-AC	Chemviron Carbon	0.6245	4.613	1.0554	0.0077	500	-
GRANULAR CARBON							
208C	Chemviron Carbon	0.3077	4.4390	1.187	0.0100	510	Coco Shell
607C	Chemviron Carbon	0.3475	3.5943	1.05	0.0026	500	Coco Shell
C119	Carbomafra	0.2852	3.8615	1	0.0015	512	-
SRD1352/2	Chemviron Carbon	0.8392	5.0775	0.8529	0.0150	366	Coco Shell
SRD1352/3	Chemviron Carbon	0.5691	6.6738	1.1489	0.0100	366	Coco Shell
SRD06038	Chemviron Carbon	0.4464	6.7116	1.1295	0.0100	400	Coal
SRD06039	Chemviron Carbon	0.4527	5.3630	1.053	0.0091	416	Coal
SRD06040	Chemviron Carbon	0.3483	5.5936	1.1714	0.0075	543	Coal
SRD06041	Chemviron Carbon	0.2303	5.5622	1.5252	0.0073	584	Coal
CARBON FIBRE & CLOTH							
ACF CC200	Chemviron Carbon	0.3040	4.611	1.468	0.0010	300	Polymer
ACF CC250	Chemviron Carbon	0.3150	5.569	1.602	0.0010	300	Polymer
FM10/700	Chemviron Carbon	0.4489	5.9276	1.148	0.0010	384	Polymer
ACF-20	Osaka Gas Chemical	0.7817	4.4783	0.7573	0.0100	104	-
CARBON POWDER							
C-2132	Westvaco	0.9258	4.1005	0.85	0.0206	280	Coal
AX-21	Andersen	0.549	9.078	2	0.0100	250	Coal
MSC-30	Kansai	1.0595	5.6621	0.8115	0.0033	260	Coal
COMPACTED SAMPLES							
208C	Chemviron Carbon	0.3077	4.439	1.187	0.0100	770	Coco Shell
SRD1352/2	Chemviron Carbon	0.8392	5.0775	0.8529	0.0150	435	Coco Shell
FM10/700	Chemviron Carbon	0.4489	5.9276	1.148	0.0010	529	Polymer
ACF-20	Osaka Gas Chemical	0.7817	4.4783	0.7573	0.0100	294	-

Coco Shell = Coconut Shell

Table 1: Carbon adsorbent characteristics

SIMULATION RESULTS

Ice making applications ($T_C = 35^\circ\text{C}$, $T_E = -5^\circ\text{C}$ and $T_1 = 35^\circ\text{C}$)

Monolithic carbon

The results are shown in **Figure 6**. For single bed and two-beds, the sample KOH-AC gives the highest COP (0.46 and 0.67 for single bed and two-beds, respectively, with a driving temperature of 200°C) while the sample LM001 gives the lowest COP (0.36 and 0.55 for single bed and two-beds, respectively, with a driving temperature of 200°C). From single to two-beds, there is an improvement in COP of up to 30%. Considering the ideal case (an infinite number of beds and ideal heat transfer), the COP could double ($\text{COP}\sim 0.75$) at lower and medium driving temperature or triple ($\text{COP}\sim 1.5$) at the higher driving temperatures ($170^\circ\text{C} < T_3 < 200^\circ\text{C}$); the difference in COP between the monolithic carbons tested is marginal. The cooling production ranges from 5 MJ m^{-3} to 230 MJ m^{-3} . The KOH-AC-ammonia pair gives the best cooling production: 66 MJ m^{-3} ($T_3=100^\circ\text{C}$) and 228 MJ m^{-3} ($T_3=200^\circ\text{C}$). The LM001-ammonia pair gives the lowest cooling production: 39 MJ m^{-3} ($T_3=100^\circ\text{C}$) and 108 MJ m^{-3} ($T_3=200^\circ\text{C}$).

Granular carbon

Figure 7 shows the simulation results for various granular carbons. For a single bed and two-beds, the sample SDR 1352/2 and SRD1352/3 give the highest COP (0.46 and 0.67 for single bed and double bed respectively with a driving temperature of 200°C) while the sample C119 shows the lowest COP (0.34 and 0.53 for a single bed and two-beds, respectively, with a driving temperature of 200°C). From single to two-beds, there is an improvement in COP of up to 35%. With the ideal case the COP could double ($\text{COP}\sim 0.80$) at lower and medium driving temperature or triple ($\text{COP}\sim 1.3$ with SRD1352/2) or quadruple ($\text{COP}\sim 1.6$ with SRD06041) at higher driving temperature ($170^\circ\text{C} < T_3 < 200^\circ\text{C}$). The cooling production ranges from 4 MJ m^{-3} to 106 MJ m^{-3} . The SRD1352/2-ammonia pair gives the highest cooling production: 36 MJ m^{-3} ($T_3=100^\circ\text{C}$) and 106 MJ m^{-3} ($T_3=200^\circ\text{C}$). The C119-ammonia pair gives the lowest cooling production: 19 MJ m^{-3} ($T_3=100^\circ\text{C}$) and 70 MJ m^{-3} ($T_3=200^\circ\text{C}$).

Carbon fibre and cloth

The carbon cloth FM10/700 and carbon fibre ACF-20 have fairly similar COP and best value when considering both single and two-bed cycles: 0.43 and 0.63 for single bed and two-beds respectively with a driving temperature of 200°C (**Figure 8**). From single to two-bed, there is an improvement in COP of up to 33%. With the ideal case the COP could double ($\text{COP}\sim 0.80$) at lower and medium driving temperature or triple ($\text{COP}\sim 1.3$ with the carbon cloth FM10/700 and carbon fibre ACF-20) or quadruple ($\text{COP}\sim 1.7$ with the carbon cloth CC200 and C250) at higher driving temperature ($170^\circ\text{C} < T_3 < 200^\circ\text{C}$). The cooling production varies from 2 MJ m^{-3} to 90 MJ m^{-3} . The carbon cloth FM10/700-ammonia pair gives the highest cooling production: 27 MJ m^{-3} ($T_3=100^\circ\text{C}$) and 83 MJ m^{-3} ($T_3=200^\circ\text{C}$). The carbon fibre ACF-20-ammonia pair gives the lowest cooling production: 8 MJ m^{-3} ($T_3=100^\circ\text{C}$) and 25 MJ m^{-3} ($T_3=200^\circ\text{C}$).

Carbon powder

The carbon powders tested are highly activated as carbon fibre and cloth samples and globally present fairly similar figures of COP. The best value when considering both single and double bed configuration: 0.45 and 0.72 for single bed and double bed, respectively, with a driving temperature of 200°C for the AX-21 (**Figure 9**). The cooling production varies from 4 MJ m^{-3} to 112 MJ m^{-3} . The carbon powder C-2132-ammonia pair gives the highest cooling production up to a driving temperature of about 140°C (70 MJ m^{-3}) while beyond 140°C the carbon powder AX-21-ammonia pair is better (111 MJ m^{-3} with $T_3=200^\circ\text{C}$).

Compacted samples of carbon

The COP of the compacted samples is unchanged since it is mainly driven by ammonia uptake (kg ammonia/kg carbon). However, the cooling production for a given sample is

directly proportional to its density. The density improvements are about 16% with SRD1232/2, 27% with FM10/700, 33% with 208C and 65% with ACF-20: the cooling production improvement with each compacted sample will follow the same trend. The compacted granular carbon 208C-ammonia pair presents globally the best cooling production with a maximum of 132 MJ m^{-3} with a driving temperature of 200°C (**Figure 10**).

Both COP and cooling production increase with the bed driving temperature as expected. For the ice making application and regardless of the type of carbon sample, the need to use a high driving temperature beyond 120°C to 140°C depends on the heat source. For 'free' heat source such as solar, agricultural or industrial waste, the cooling production is the main figure of merit and any cooling gained at high driven temperature is appreciated. However, with a gas-fired heat source, the COP is critical and performance benefits must be significant to justify use of driving temperatures beyond 120°C to 140°C . With the exception of the monolithic SDS (up to 17% increase) no other samples tested seems appropriate for use above 140°C with one bed, as the COP increases remain marginal (less than 7%). With a two-bed cycle, it will be useful to operate beyond 140°C driving temperature since the increase in COP could be substantial (up to 15%).

Air conditioning applications ($T_C = 35^\circ\text{C}$, $T_E = 10^\circ\text{C}$ and $T_1 = 35^\circ\text{C}$)

Monolithic carbon

The results are shown in **Figure 11**. For a single bed and two-beds, the sample KOH-AC gives the highest COP (0.52 and 0.85 for single bed and two-bed, respectively, with a driving temperature of 200°C) while the monolithic sample SDS gives the lowest COP (0.39 and 0.66 for single bed and double bed, respectively, with a driving temperature of 200°C). From single to two-beds, there is an improvement in COP of up to 40%. Considering the ideal case, the COP could increase by up to a factor of nine ($\text{COP}_{\text{Single}} \sim 0.41$ and $\text{COP}_{\text{ideal}} \sim 3.6$ with LM001 at $T_3 = 200^\circ\text{C}$). The cooling production ranges from 25 MJ m^{-3} to 320 MJ m^{-3} . The KOH-AC-ammonia pair gives the highest cooling production: 151 MJ m^{-3} ($T_3 = 100^\circ\text{C}$) and 316 MJ m^{-3} ($T_3 = 200^\circ\text{C}$). The LM001-ammonia pair gives globally the lowest cooling production: 60 MJ m^{-3} ($T_3 = 100^\circ\text{C}$) and 141 MJ m^{-3} ($T_3 = 200^\circ\text{C}$).

Granular carbon

Figure 12 shows the simulation results with various granular carbons. For a single bed and two-bed, the sample SRD1352/2 gives the highest COP (0.55 and 0.87 for single bed and two-beds, respectively, with a driving temperature of 200°C) while the sample SRD06041 gives the lowest COP (0.42 and 0.70 for single bed and two-bed respectively with a driving temperature of 200°C). From single to two-bed, there is an improvement in COP of up to 37%. In the ideal case the COP could increase by a factor of ten ($\text{COP}_{\text{Single}} \sim 0.41$ and $\text{COP}_{\text{ideal}} \sim 4.1$ with SRD06041 at $T_3 = 200^\circ\text{C}$). The cooling production ranges from 28 MJ m^{-3} to 162 MJ m^{-3} . The SRD1532/2-ammonia pair gives the highest cooling production: 91 MJ m^{-3} ($T_3 = 100^\circ\text{C}$) and 162 MJ m^{-3} ($T_3 = 200^\circ\text{C}$). The C119-ammonia pair gives the lowest cooling production: 43 MJ m^{-3} ($T_3 = 100^\circ\text{C}$) and 94 MJ m^{-3} ($T_3 = 200^\circ\text{C}$).

Carbon fibre and cloth

The carbon cloth FM10/700 and carbon fibre ACF-20 have similar COP and highest value are 0.51 and 0.84 for single bed and two-bed, respectively, with a driving temperature of 200°C (**Figure 13**). From single to two-bed, there is an improvement in COP of up to 40%. In the ideal case the COP could increase by a factor of ten ($\text{COP}_{\text{Single}} \sim 0.43$ and $\text{COP}_{\text{ideal}} \sim 4.3$ with CC200 at $T_3 = 200^\circ\text{C}$). The cooling production varies from 15 MJ m^{-3} to 125 MJ m^{-3} . The carbon cloth FM10/700-ammonia pair gives the highest cooling production: 62 MJ m^{-3} ($T_3 = 100^\circ\text{C}$) and 122 MJ m^{-3} ($T_3 = 200^\circ\text{C}$). The carbon fibre ACF-20-ammonia pair gives the lowest cooling production: 21 MJ m^{-3} ($T_3 = 100^\circ\text{C}$) and 38 MJ m^{-3} ($T_3 = 200^\circ\text{C}$).

Carbon powder

The highest values of COP are 0.45 and 0.72 for single bed and two-bed, respectively, with a driving temperature of 200°C for the AX-21 (**Figure 14**). From single to two-bed, the COP improvement is up to 36%. With the ideal cycle, the COP could increase by up to a factor of seven ($COP_{\text{Single}} \sim 0.54$ and $COP_{\text{ideal}} \sim 3.6$ with AX-21 at $T_3 = 200^\circ\text{C}$). The cooling production varies from 20 MJ m⁻³ to 150 MJ m⁻³. The carbon powder C-2132-ammonia pair gives the highest cooling production: 74 MJ m⁻³ ($T_3 = 100^\circ\text{C}$) and 145 MJ m⁻³ ($T_3 = 200^\circ\text{C}$).

Compacted samples of carbon

As with the ice making application, the COP of the compacted samples is unchanged since it is mainly driven by ammonia uptake (kg ammonia/kg carbon). The cooling production improvement with each compacted sample will also follow the same trend as the density improvement (16% with SRD1232/2, 27% with FM10/700, 33% with 208C and 65% with ACF-20). The compacted granular carbon SRD1232/2-ammonia pair presents the best cooling production with a maximum of 192 MJ m⁻³ with a driving temperature of 200°C (**Figure 15**).

As with the ice making applications, both COP and cooling production also increase with the bed driving temperature as expected. Considering a single bed or two-bed cycle and with the exception of the monolithic SDS (up to 20% of $COP_{\text{Double bed}}$ increase), the variation of COP is marginal beyond a driving temperature of about 140°C (less than a 7% COP increase). Unless the heat source is free, it will not be useful to operate beyond a driving temperature of about 140°C unless there is a substantial gain in cooling production (e.g. for the monolithic carbon KOH-AC: about 20% cooling production gain from 140°C to 200°C driving temperature).

Heat pump applications ($T_C = 40^\circ\text{C}$, $T_E = 5^\circ\text{C}$ and $T_1 = 40^\circ\text{C}$)

Monolithic carbon

For single bed and two-bed cycles, the sample KOH-AC gives the highest COP (1.50 and 1.70 for single bed and two-bed, respectively, with a driving temperature of 200°C) while the sample SDS gives the lowest COP (1.36 and 1.56 for single bed and two-bed, respectively, with a driving temperature of 200°C) as shown in **Figure 16**. From single to two-bed, there is an improvement in COP of up to 30%. Considering the ideal case, the COP could double ($COP \sim 3$) at higher driving temperature ($170^\circ\text{C} < T_3 < 200^\circ\text{C}$); the difference in COP between the monolithic carbons tested is globally marginal. The heating production ranges from 10 MJ m⁻³ to 800 MJ m⁻³. The KOH-AC-ammonia pair gives the highest heating production: 237 MJ m⁻³ ($T_3 = 100^\circ\text{C}$) and 594 MJ m⁻³ ($T_3 = 200^\circ\text{C}$) with a two-bed cycle. The LM001-ammonia pair gives the lowest heating production: 113 MJ m⁻³ ($T_3 = 100^\circ\text{C}$) and 308 MJ m⁻³ ($T_3 = 200^\circ\text{C}$) with a two-bed cycle.

Granular carbon

Figure 17 shows the simulation results with various granular carbons. For single bed and two-bed, the sample SRD1352/2 gives the highest COP (1.51 and 1.73 for single bed and two-bed, respectively, with a driving temperature of 200°C) while the sample SRD06041 gives the lowest COP (1.38 and 1.59 for single bed and two-bed, respectively, with a driving temperature of 200°C). From single to two-bed, there is an improvement in COP of up to 13%. With the ideal case, the COP could double. The heating production ranges from 14 MJ m⁻³ to 370 MJ m⁻³. The SRD1352/2-ammonia pair gives the highest heating production: 128 MJ m⁻³ ($T_3 = 100^\circ\text{C}$) and 287 MJ m⁻³ ($T_3 = 200^\circ\text{C}$) with double bed configuration. The C119-ammonia pair gives the lowest cooling production: 80 MJ m⁻³ ($T_3 = 100^\circ\text{C}$) and 206 MJ m⁻³ ($T_3 = 200^\circ\text{C}$) with a two-bed cycle.

Carbon fibre and cloth

The carbon cloth FM10/700 and carbon fibre ACF-20 have fairly close COP and the highest values are 1.46 and 1.69 for single bed and two-bed, respectively, with a driving temperature

of 200°C (**Figure 18**). From single to two-bed, there is an improvement in COP of up to 14%. With the ideal case, the COP could double. The heating production varies from 8 MJ m⁻³ to 310 MJ m⁻³. The carbon cloth FM10/700-ammonia pair gives the highest heating production: 97 MJ m⁻³ ($T_3=100^\circ\text{C}$) and 235 MJ m⁻³ ($T_3=200^\circ\text{C}$) with a two-bed cycle. The carbon fibre ACF-20-ammonia pair gives the lowest heating production: 31 MJ m⁻³ ($T_3=100^\circ\text{C}$) and 70 MJ m⁻³ ($T_3=200^\circ\text{C}$) with a two-bed cycle.

Carbon powder

The highest values of COP are 1.50 and 1.8 for single bed and two-bed, respectively, with a driving temperature of 200°C and are obtained with the AX-21 (**Figure 19**). The heating production varies from 14 MJ m⁻³ to 336 MJ m⁻³. The carbon powder C-2132-ammonia pair gives the highest heating production: 110 MJ m⁻³ ($T_3=100^\circ\text{C}$) and 262 MJ m⁻³ ($T_3=200^\circ\text{C}$) with a two-bed cycle.

Compacted samples of carbon

As with the ice making and air conditioning applications, the COP of the compacted samples is unchanged since it is mainly driven by ammonia uptake (kg ammonia/kg carbon). The heating production improvement with each compacted sample will also follow approximately the same trend as the density improvement (16% with SRD1232/2, 27% with FM10/700, 33% with 208C and 65% with ACF-20). The compacted granular carbon 208C-ammonia pair presents globally the best heating production with maximum values of 501 MJ m⁻³ and 368 MJ m⁻³ with a driving temperature of 200°C for single bed and two-bed cycles, respectively (**Figure 20**).

Regardless of the type of carbon tested, both COP and heating production increase with the bed driving temperature as expected since they are all driven by the variation of ammonia uptake in the bed (**Figure 16**, **Figure 17**, **Figure 18**, **Figure 19** and **Figure 20**). Globally the COP varies from 1 to 3.5 while the heating production ranges from 5 MJ m⁻³ (infinite number of beds) to 800 MJ m⁻³ (Single bed). Considering a single bed configuration, the variation of COP is marginal beyond a driving temperature of about 120°C to 140°C (less than a 6% COP increase). Unless the heat source is free, it will not be useful to operate beyond a driving temperature of about 140°C (with single or two-bed cycles).. With an infinite number of beds (Ideal), the COP varies little with driving temperature up to about 120°C and has an average value of about 1.8 which is independent of the sample. The heating production decreases with the number of beds as expected, since COP increases and less heat is externally rejected during adsorption.

With an ideal cycle (infinite number of beds) and for all three applications investigated (ice making, air conditioning and heat pumping), the ideal COP depends only on the driving temperature (T_3) and is independent of the sample until a tipping temperature. At this temperature the COP starts to increase sharply with increased driving temperature and there is divergence between the COPs of the carbon samples. The tipping temperature (T_{tip}) corresponds to the driving temperature at which $T_2 = T_4$ as illustrated in both **Figure 2** and **Figure 5** and is given by:

$$T_{tip} = \left(\frac{T_C}{T_E} \right)^2 T_1 \quad (15)$$

This driving temperature defines the driving temperature above which some part of the heat of adsorption can be recovered to provide some of the heat of desorption, therefore reducing the heat input required for the desorption process and causing the rapid increase in the COP

above this temperature. This tipping temperature is calculated for the three applications in **Table 2**.

	Ice making	Air conditioning	Heat pumping
T_E ($^{\circ}C$)	-5	10	5
T_C ($^{\circ}C$)	35	35	40
T_1 ($^{\circ}C$)	35	35	40
$T_2 = T_4$ ($^{\circ}C$)	81	62	80
T_{tip} ($^{\circ}C$)	134	92	124

Table 2: Tipping temperatures for the three applications

Below the tipping temperature, only the sensible heat of the bed can be recovered to provide some of the heat of desorption as illustrated in **Figure 21** for carbon 208C in the air conditioning application with a driving temperature of 85°C. The external heat input to the cycle Q_{input} is given by the area of the hatch-marked region which has been split into two sections Q_{hot1} and Q_{hot2} .

The heat input Q_{hot1} is required due to the lower ammonia concentration in the bed during the depressurisation stage than during the pressurisation stage of the cycle (and therefore a lower bed heat capacity), and is given by:

$$Q_{hot1} = \Delta x c_{pa} (T_2 - T_4) \quad (16)$$

At low driving temperatures, the temperature-concentration characteristics for the carbons is extremely linear as illustrated in **Figure 22** for two of the carbon samples. This means that if the gas constant R can be assumed constant at the condensing pressure P_C between temperatures T_2 and T_3 then the following simplified expression can be derived for Q_{hot2} :

$$Q_{hot2} = R \frac{\frac{1}{2}(T_2 + T_3)}{T_c} A \Delta x + \frac{\Delta x}{2} (T_3 - T_2) c_{pa} \quad (17)$$

$Q_{input} = Q_{hot1} + Q_{hot2}$ is therefore directly proportional to the concentration change Δx . The cooling produced, Q_c , is also proportional to the concentration change as given by equation (4) and therefore the COP is independent of the carbon in this region.

Beyond the tipping temperature, the external heat input is illustrated by the hatch-marked area in **Figure 23** for the air conditioning application for 208C. The heat of adsorption can be used to provide some of the heat of desorption between temperatures T_2 and T_4 . It can be seen from the figure that the heat of adsorption is much lower in proportion to the heat of desorption for MSC-30 in this region than for 208C. Therefore, 208C has a higher ideal COP above the tipping temperature. This is due to the lower rate of change of concentration with temperature for MSC-30 during desorption compared to adsorption in the region between T_2 and T_4 , as illustrated in **Figure 24**.

CONCLUSION

The simulation results of various activated carbon – ammonia pairs are presented at typical conditions: $T_C = 35^{\circ}C$, $T_E = -5^{\circ}C$ and $T_1 = 35^{\circ}C$ for ice making; $T_C = 35^{\circ}C$, $T_E = 10^{\circ}C$ and T_1

= 35°C for air conditioning and $T_C = 40^\circ\text{C}$, $T_E = 5^\circ\text{C}$ and $T_1 = 40^\circ\text{C}$ for heat pumping. The driving temperature T_3 varies from 80°C up to 200°C ($80^\circ\text{C} < T_3 < 200^\circ\text{C}$). The simulations were carried out for three configurations of carbon-ammonia bed: single bed, double beds and infinite number of beds. The carbon absorbents investigated are mainly coconut shell and coal based types in various shapes and sizes (monolithic, granular, compacted granular, fibre, compacted fibre, cloth, compacted cloth and powder). Considering a double bed configuration at a low driving temperature of 100°C (solar or low grade waste heat source driven machines) and a high driving temperature of 200°C (engine exhaust gas or gas-fired driven machines), the best performances are summarized in **Table 3** and **Table 4** respectively:

Samples	Ice making		Air conditioning		Heat pumping	
	q_c (MJ m ⁻³)	COP	q_c (MJ m ⁻³)	COP	q_H (MJ m ⁻³)	COP
KOH-AC (<i>monolithic</i>)	66	0.45	151	0.61	237	1.50
SRD1352/2 (Granular)	36	0.48	91	0.66	128	1.51
FM10/700 (Fibre)	27	0.48	62	0.61	97	1.47
C-2132 (Powder)	31	0.46	74	0.64	110	1.50
SRD1352/2 (Compacted)	43	0.48	108	0.66	152	1.50

Table 3: Best performance with two-bed configuration at driving temperature of 100°C.

Samples	Ice making		Air conditioning		Heat pumping	
	q_c (MJ m ⁻³)	COP	q_c (MJ m ⁻³)	COP	q_H (MJ m ⁻³)	COP
KOH-AC (<i>monolithic</i>)	228	0.68	316	0.85	594	1.70
SRD1352/2 (Granular)	106	0.67	162	0.87	287	1.70
FM10/700 (Fibre)	86	0.63	122	0.82	235	1.69
	AX-21	AX-21	C-2132	C-2132	AX-21	AX-21
(Powder)	111	0.72	145	0.88	265	1.80
	208C	208C	SRD1352/2	SRD1352/2	208C	208C
(Compacted)	132	0.58	192	0.87	368	1.62

Table 4: Best performance with two-bed configuration at driving temperature of 200°C.

ACKNOWLEDGEMENTS

This research is supported by the combined following grants:

- 1) EU SOCOOL project under the grant ENK5-CT2002-00632.
- 2) EU TOPMACS project under the grant TST4-CT-2005-012394.
- 3) EPSRC (UK-Engineering & Physical Sciences Research Council) under the grant EP/C013808/1.

The samples carbon were donated by the following individuals and companies:

- 4) Chemviron Carbons Ltd (Lockett Road, Lancashire WN4 8DE, UK).
- 5) ATMI Inc (7 Commerce Drive Danbury, CT 06810, USA).
- 6) WESTVACO (Charleston, SC 29423, USA).
- 7) Pr B.B. Saha (Institute for Materials Chemistry and Engineering, Kyushu University, Kasuga-koen 6-1, Kasuga-shi, Fukuoka 816-8580, Japan).

REFERENCES

- [1] **R. E. Critoph** - "Towards one tonne per day solar ice maker". *Proc. IVth World Renewable Energy Congress*, Denver (US), 1996, pp. 626-631.
- [2] **R. E. Critoph, Z. Tamainot-Telto and E. Munyebvu** - Solar Sorption Refrigerator - *Renewable Energy*, **12** (4) (1997), pp. 409-417.
- [3] **Z. F. Li and K. Sumathy** - A solar powered ice maker with the solid adsorption pair of activated carbon and methanol - *Int J Energy Res* **23** (1999), pp. 517-527
- [4] **A. Boubakri, J. J. Guillemot and F. Meunier** - Adsorptive solar powered ice maker: experiments and model - *Solar Energy* **69** (3) (2000), pp. 249-263.
- [5] **A. P. F. Leite and M. Daguene** - Performance of a new solid adsorption ice maker with solar energy regeneration. *Energy Conversion Mgmt* **41** (2000), pp. 1625-1647
- [6] **M. Li, R. Z. Wang, H. L. Luo, L. L. Wnag and H. B. Huang**, Experiments of a solar at plate hybrid system with heating and cooling. *Applied Thermal Engineering* **22** (2002), pp. 1445-1454.
- [7] **F. Buchter, P. H. Dind and M. Pons** - An experimental solar-powered adsorptive refrigeration tested in Burkina-Faso. *Int. J Refrigeration* **26** (2003), pp. 79-86.
- [8] **S.J. Metcalf, Z. Tamainot-Telto and R. E. Critoph** - Compact sorption generator for car and truck using waste-heat, 1rst European Mobile Air Conditioning Workshop, Paper No 05A9019, Torino, Italy, November 2005.
- [9] **R. E. Critoph, S. J. Metcalf, and Z. Tamainot-Telto** - Compact plate adsorbers for car air conditioning applications, International Heat Powered Cycles Conference (HPC 2006), Paper No 06124, Newcastle, UK, September 2006.
- [10] **S. J. Metcalf** – Gas-fired adsorption heat pump for domestic gas boiler replacement - International Heat Powered Cycles Conference (HPC 2006), Paper No 06137, Newcastle, UK, September 2006.
- [11] **F. Meunier** – Second law analysis of a solid adsorption heat pump operating on reversible cascade cycles: application to the zeolite-water pair, *Heat Recovery Systems*, **5** (1985), pp. 133-141.
- [12] **R. E. Critoph** – Adsorption refrigerators and heat pumps – Carbon materials for advanced technologies, Edited by Timothy D. Burchell, Chap. 10, pp. 303-340,1999, ISBN 0-08-042683-2

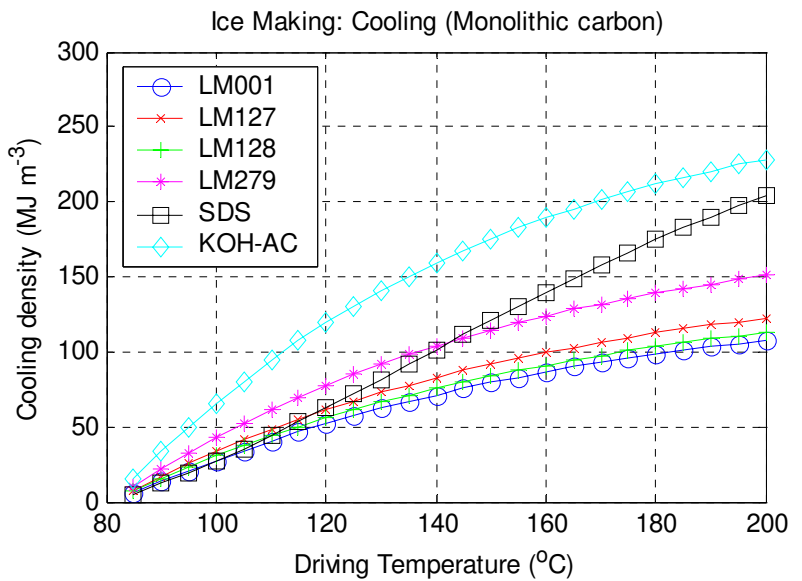
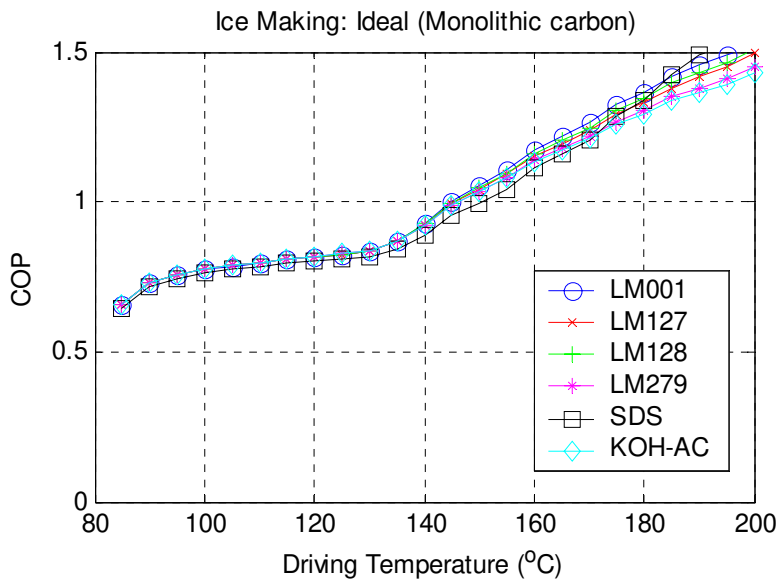
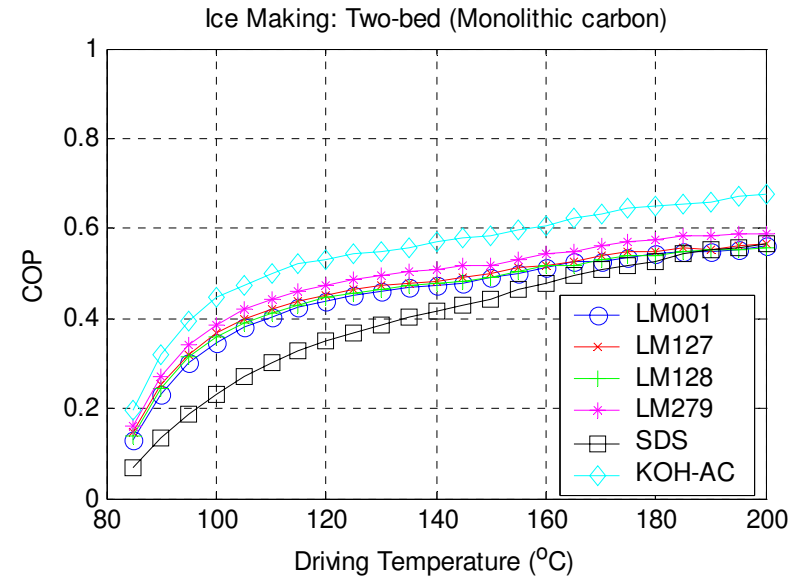
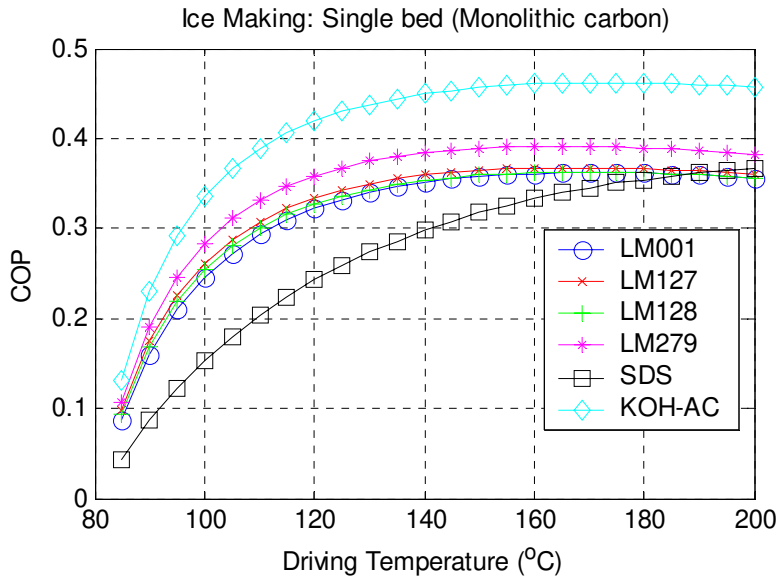


Figure 6: Ice making using monolithic carbon

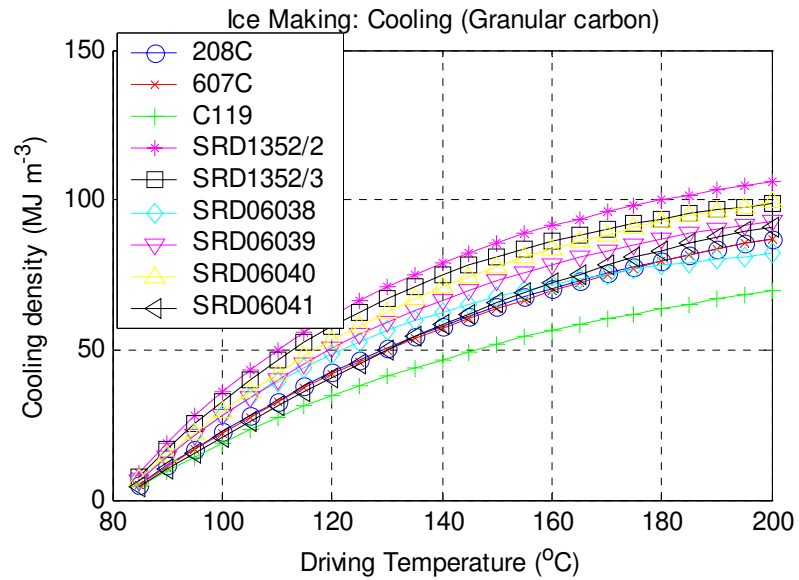
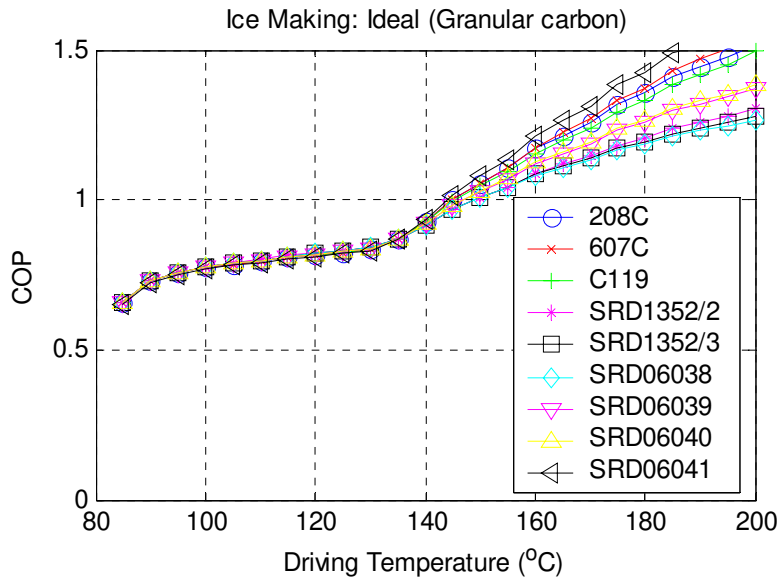
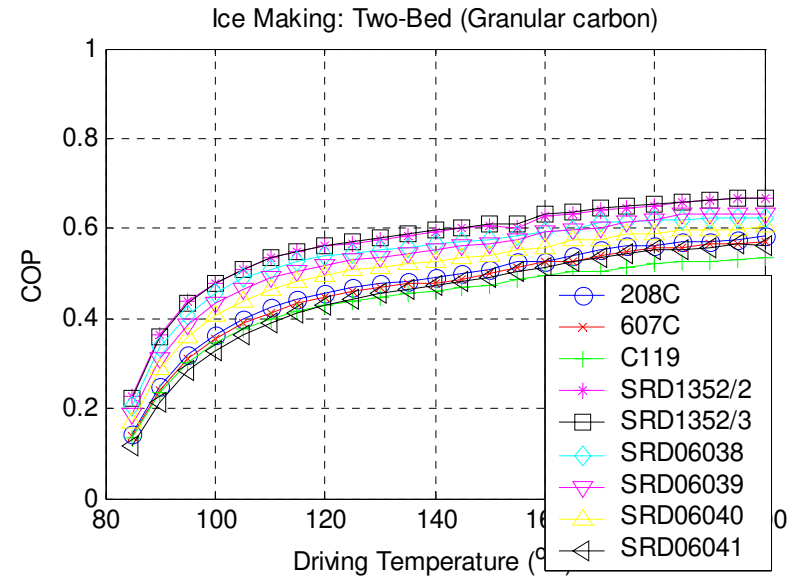
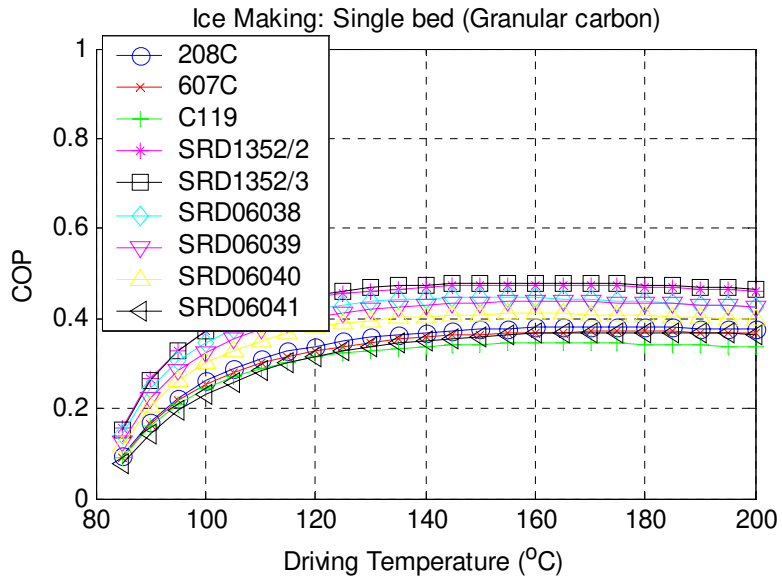


Figure 7: Ice making using granular carbon

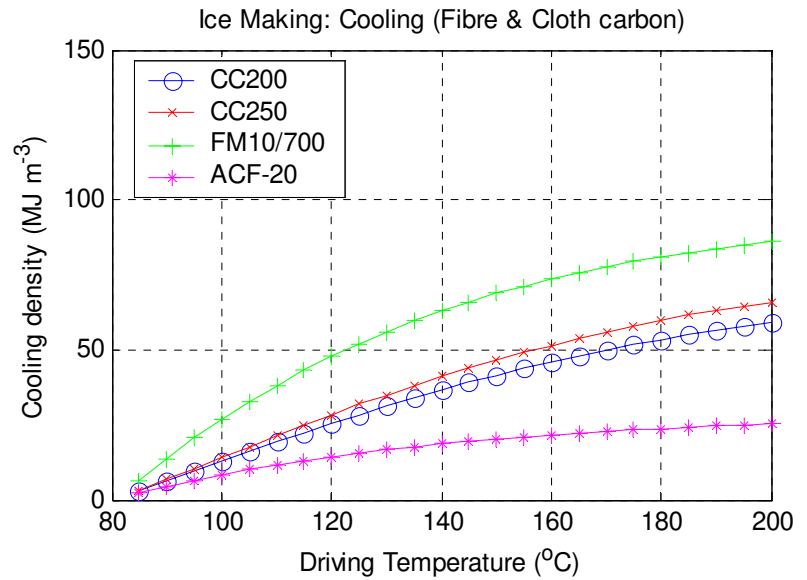
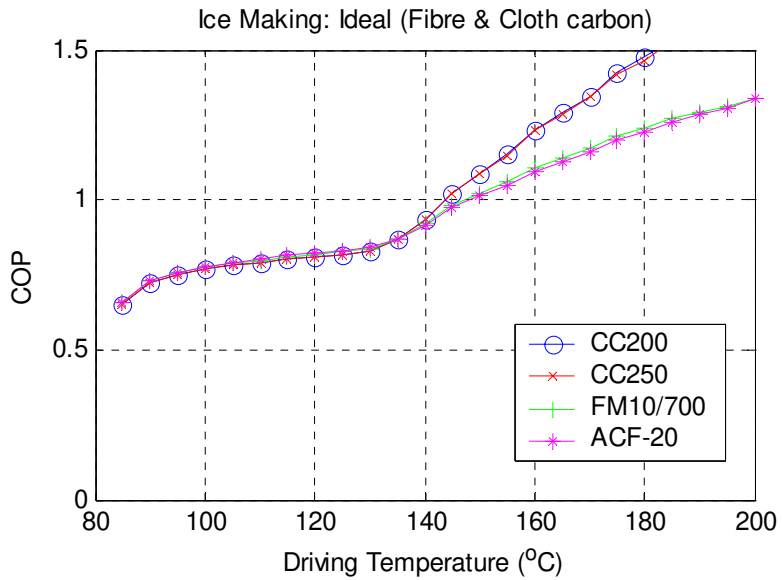
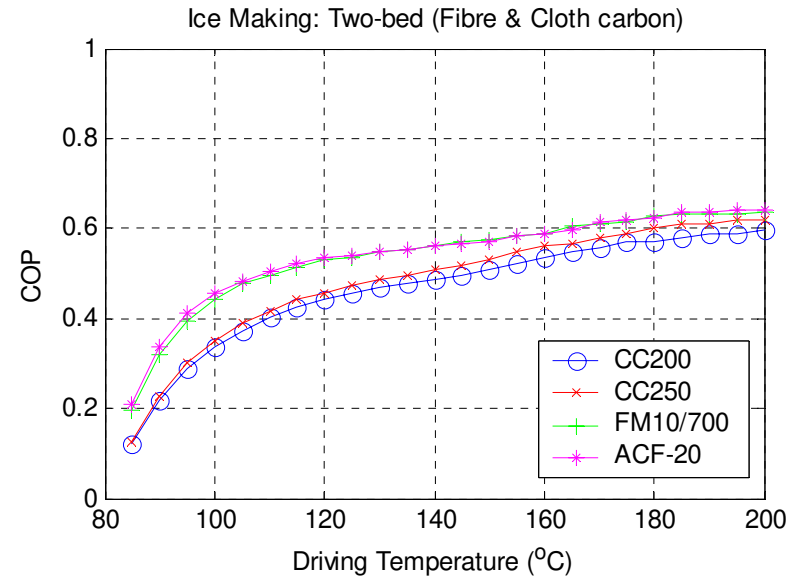
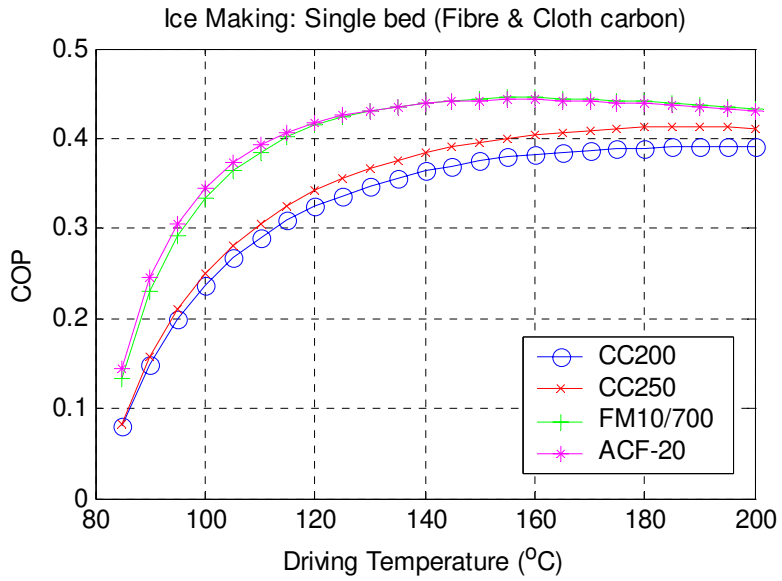


Figure 8: Ice making using carbon fibre and cloth

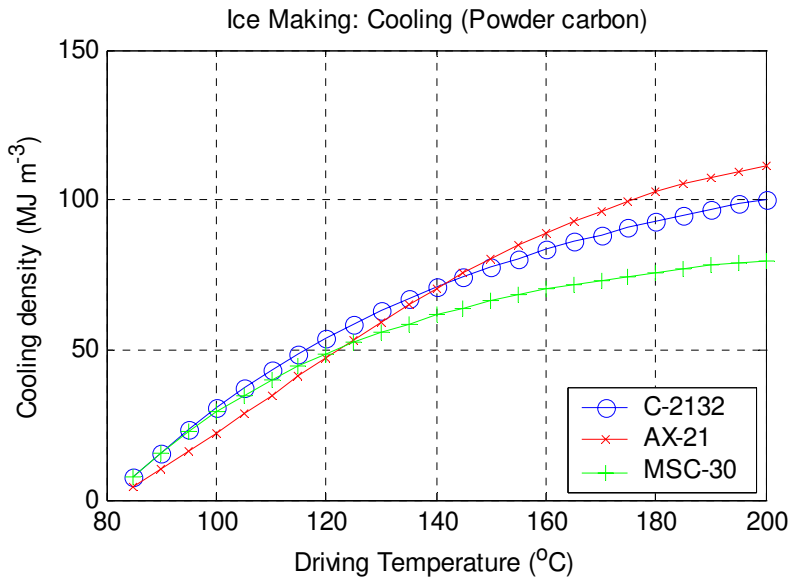
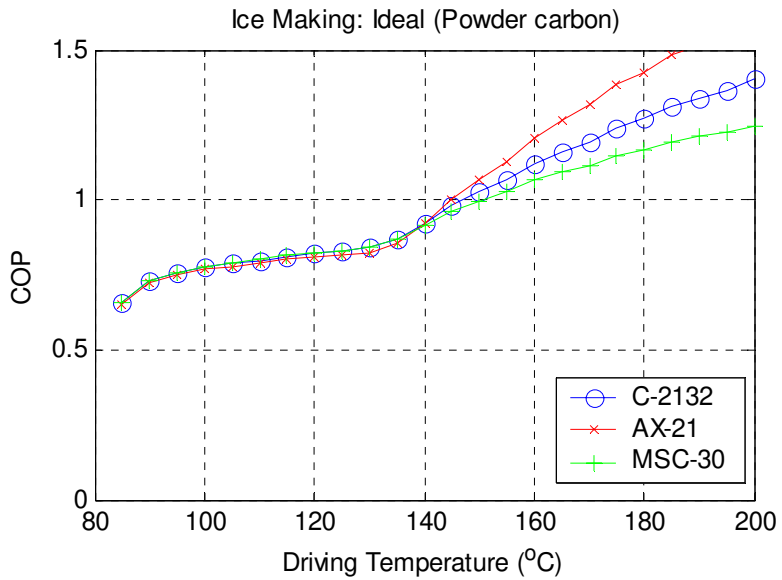
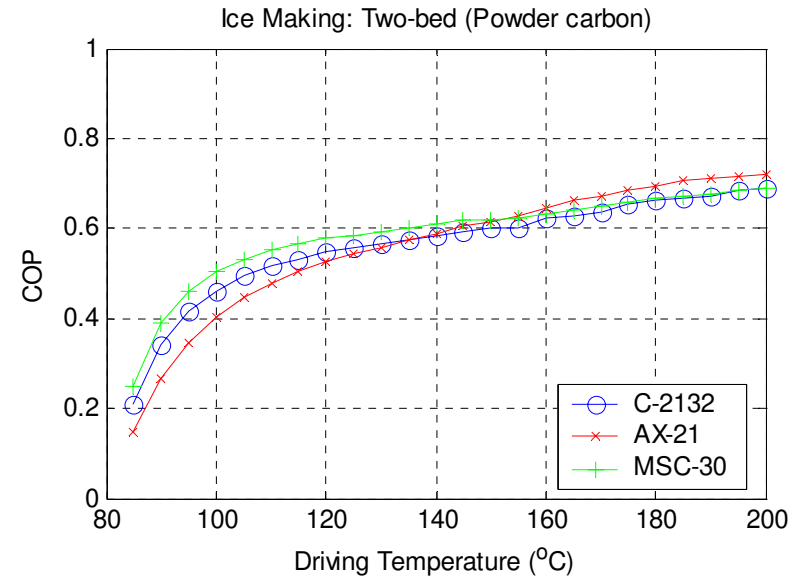
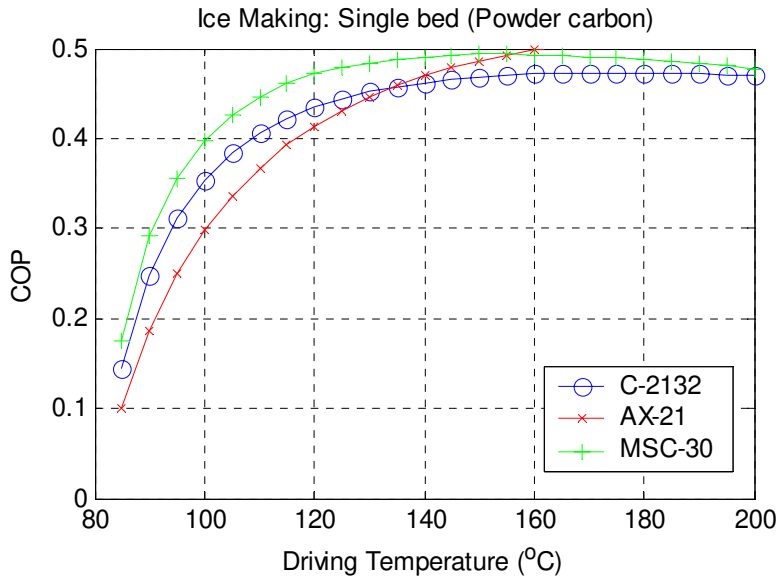


Figure 9: Ice making using carbon powder

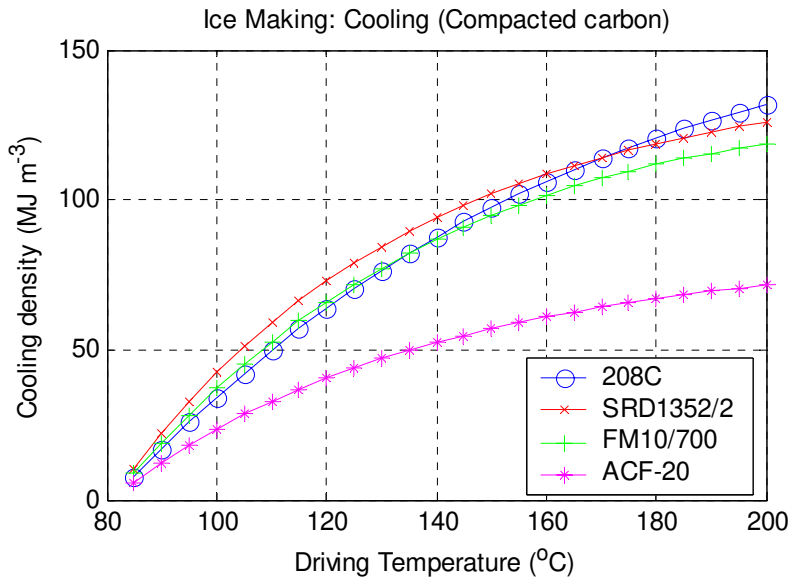
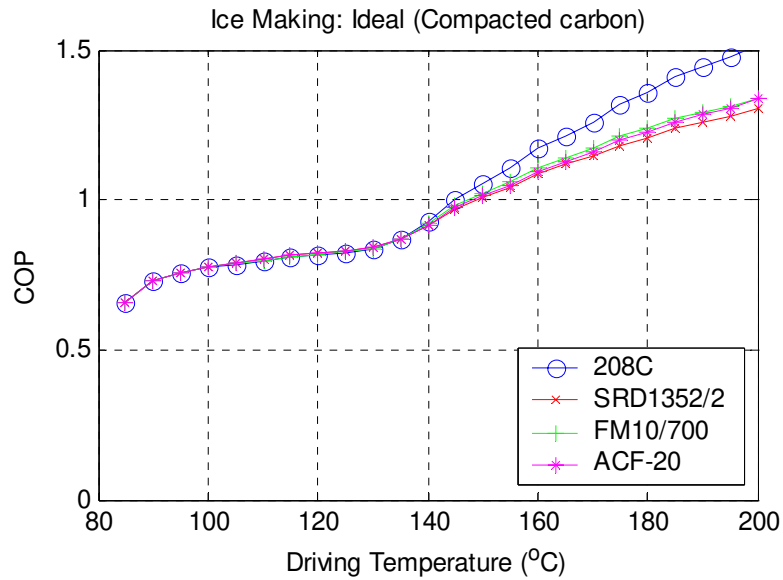
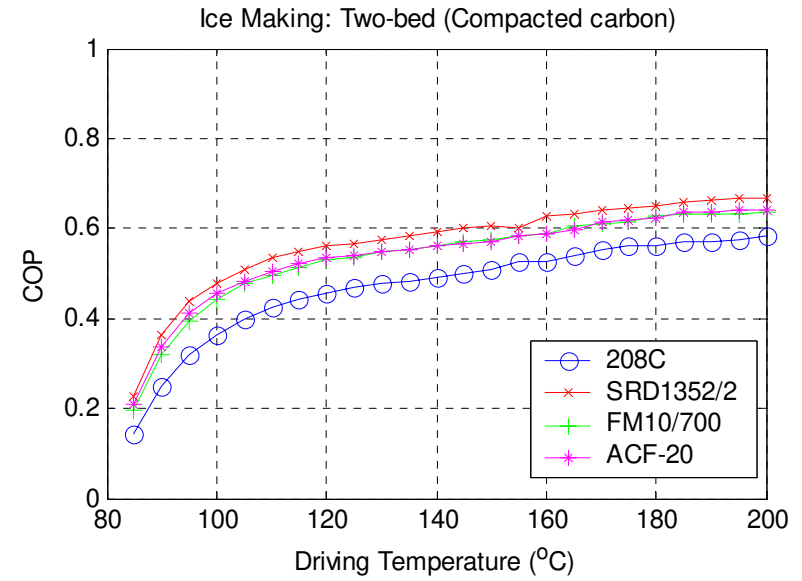
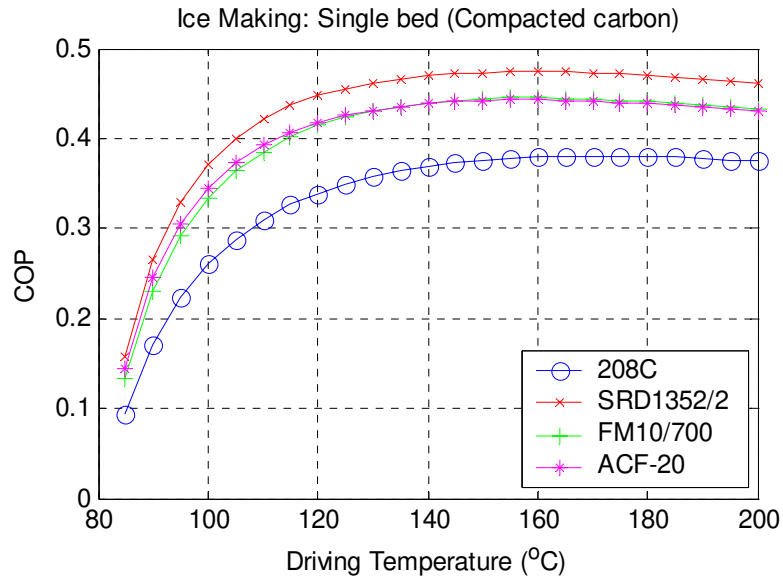


Figure 10: Ice making using compacted carbon

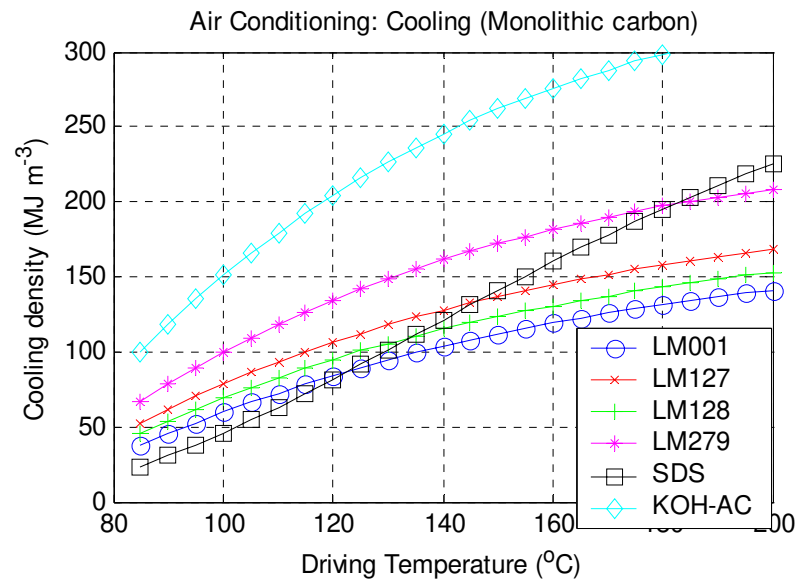
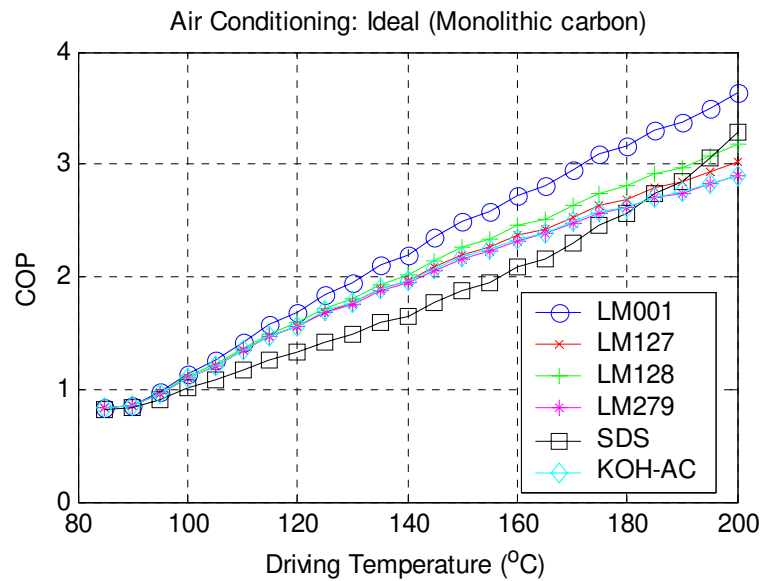
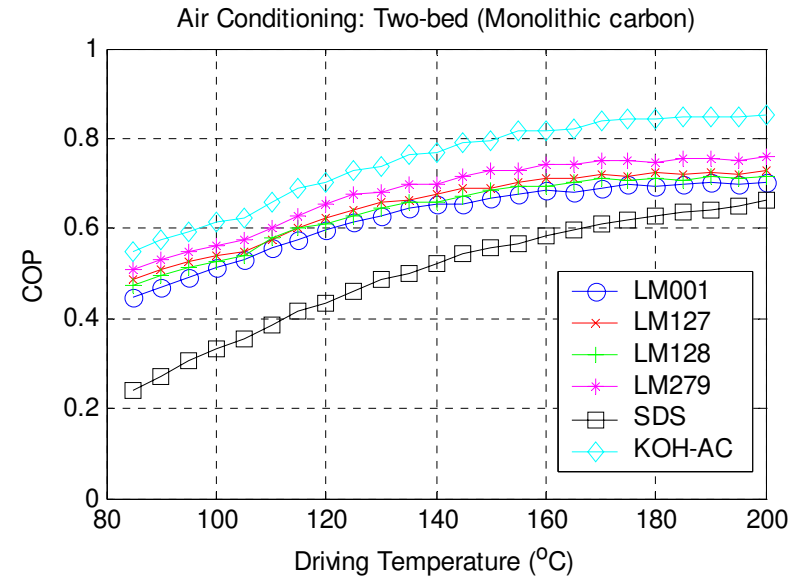
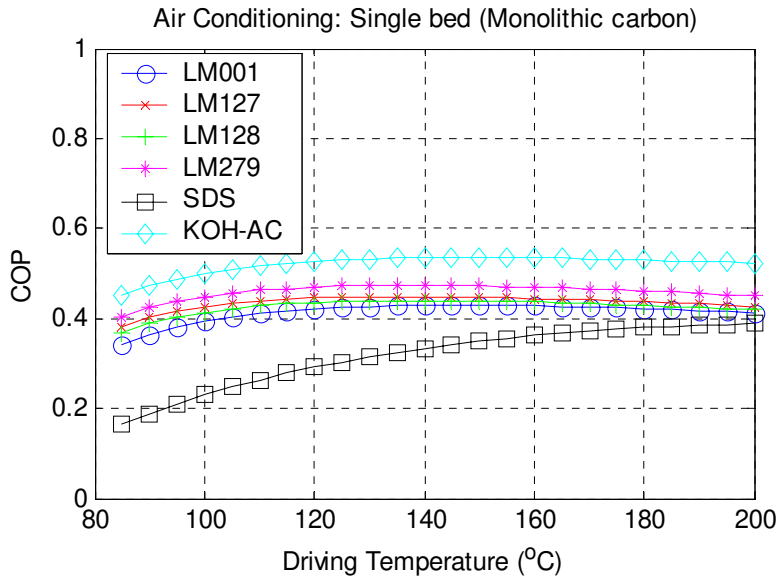


Figure 11: Air conditioning using monolithic carbon

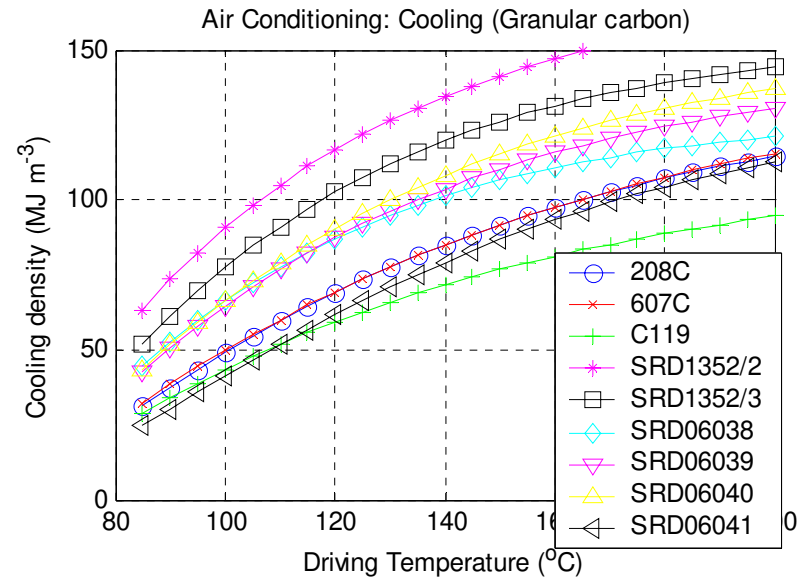
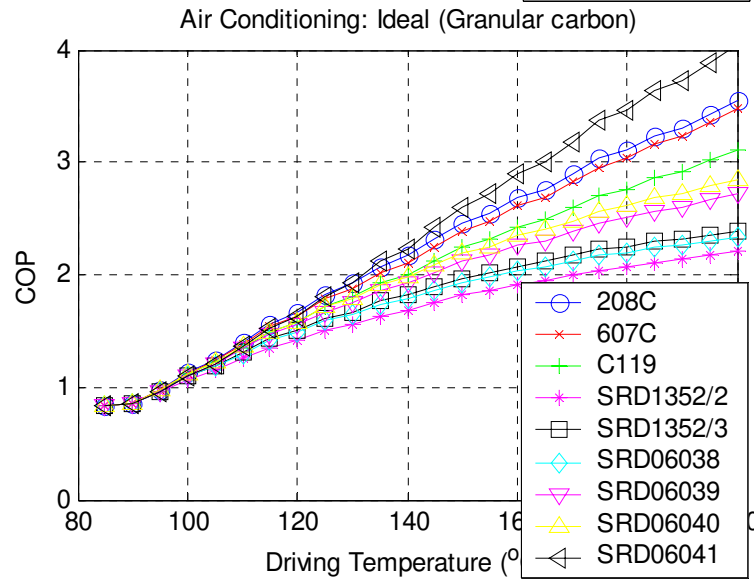
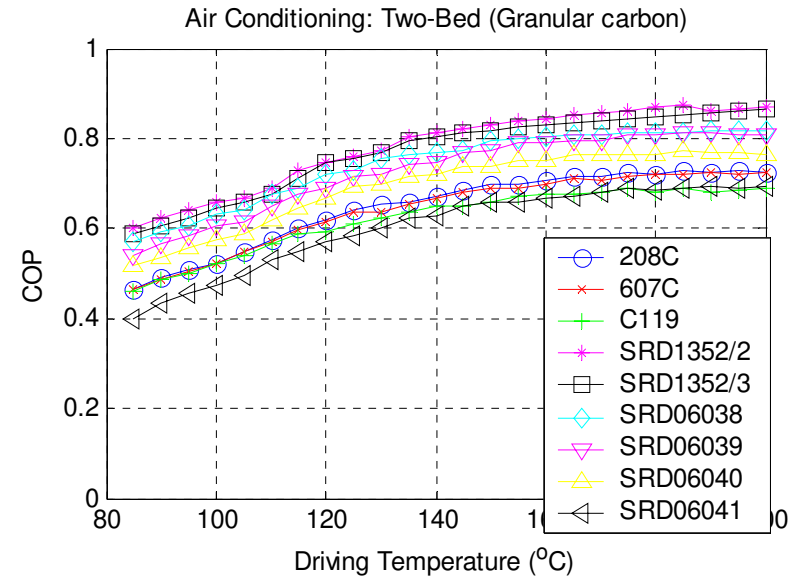
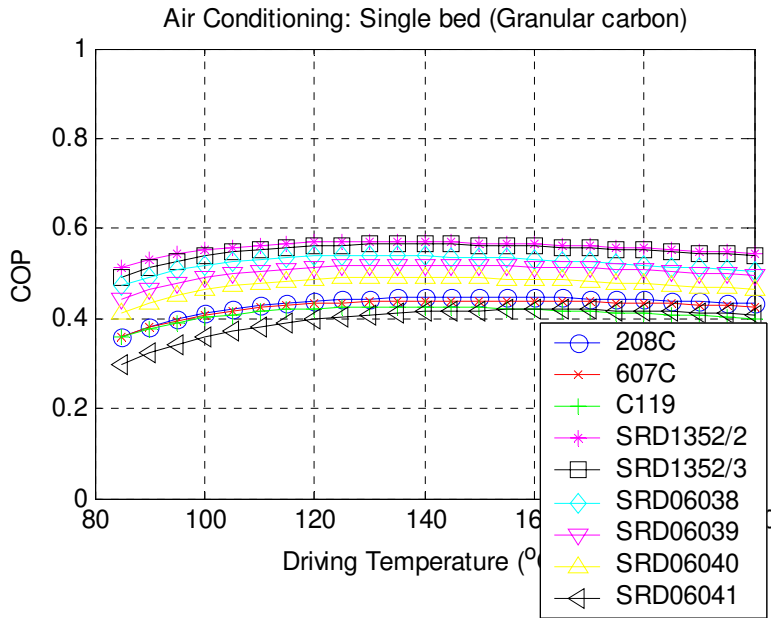


Figure 12: Air conditioning using granular carbon

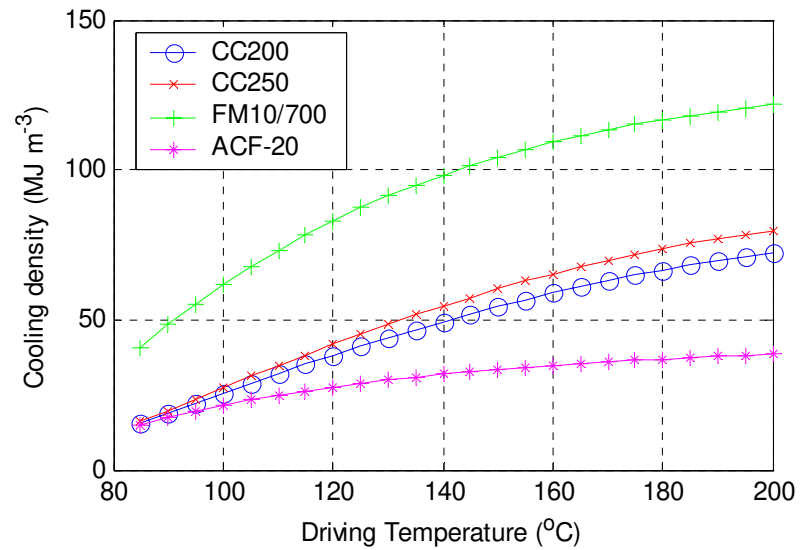
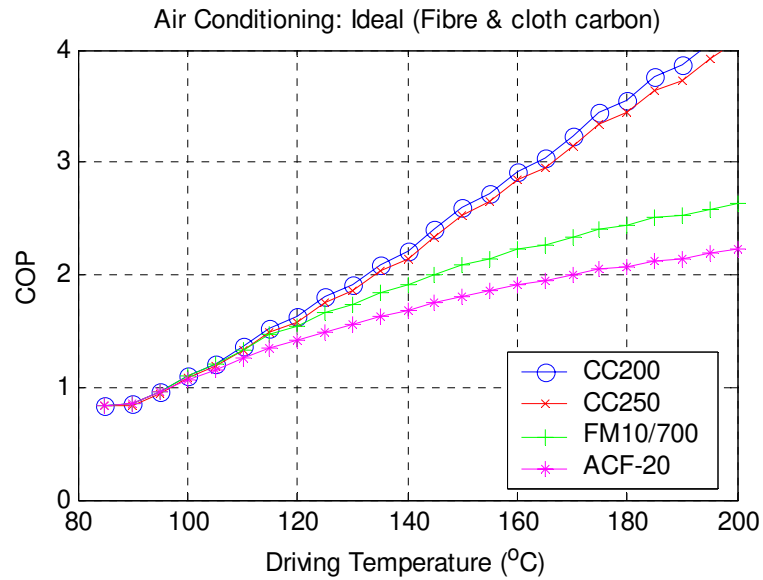
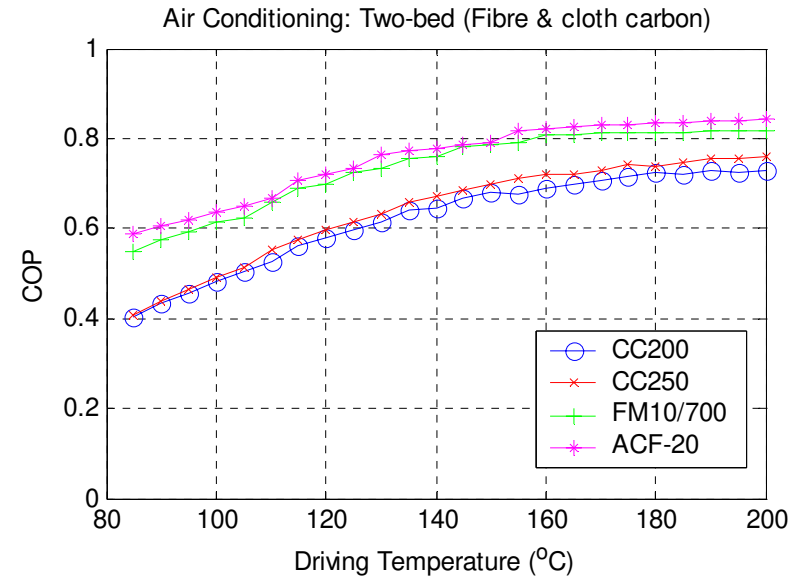
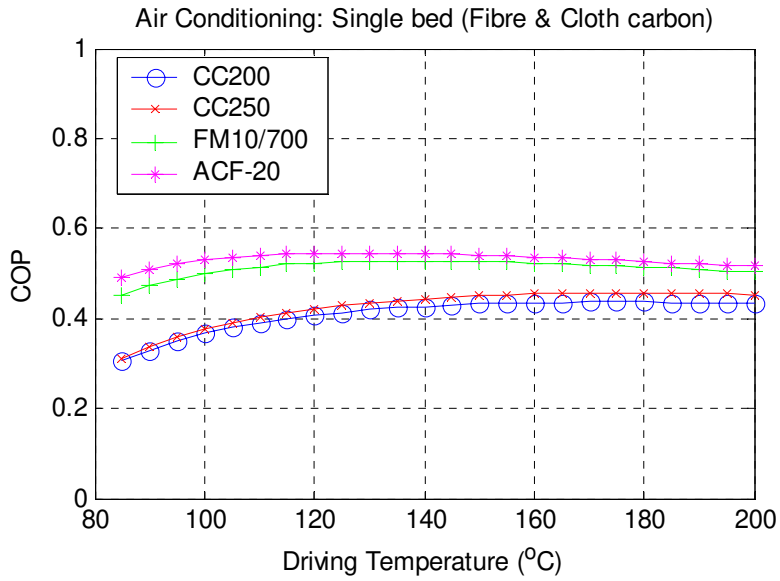


Figure 13: Air conditioning using carbon fibre and cloth

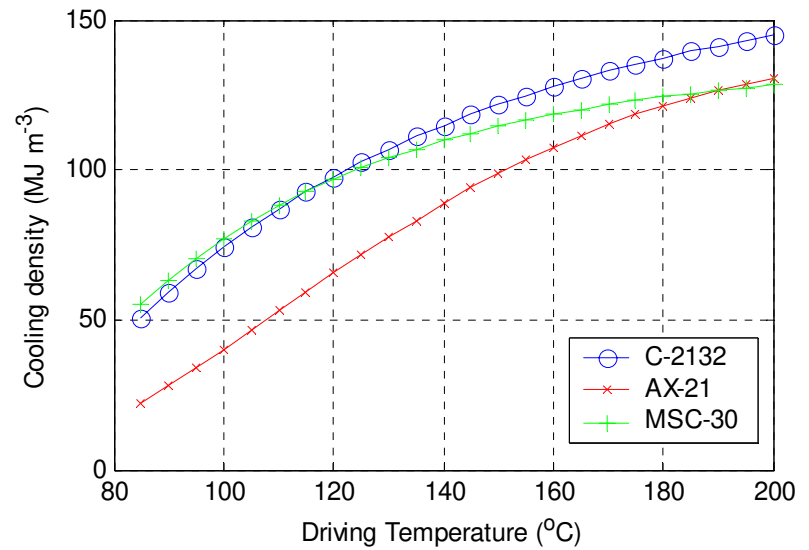
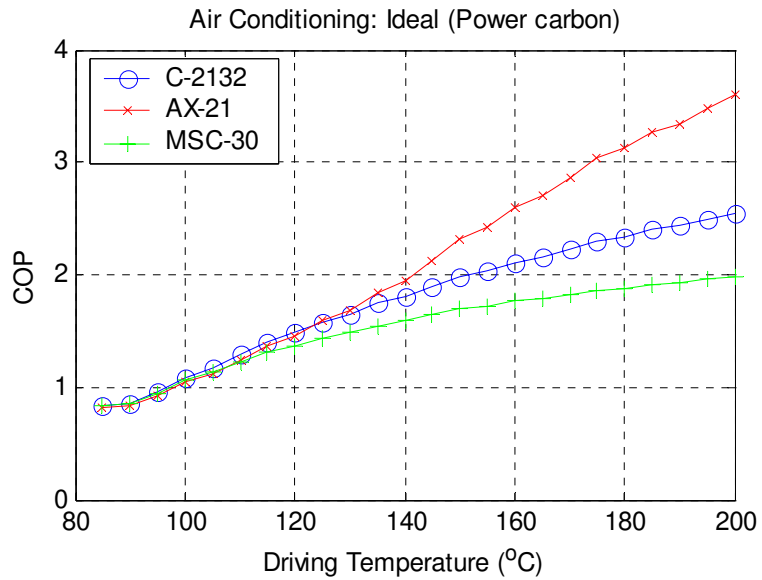
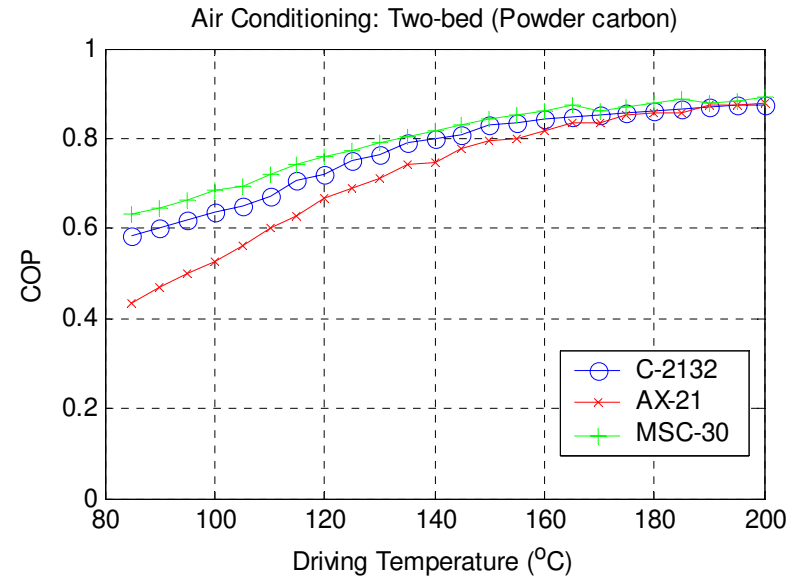
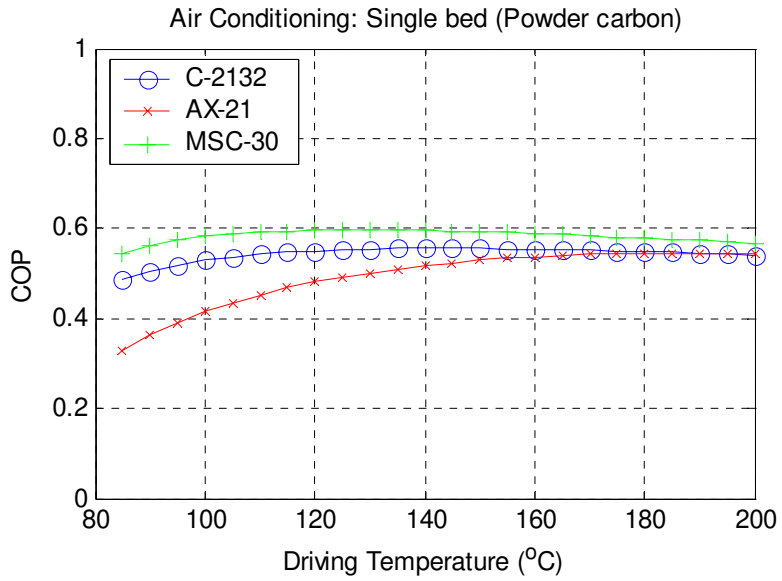


Figure 14: Air conditioning using carbon powder

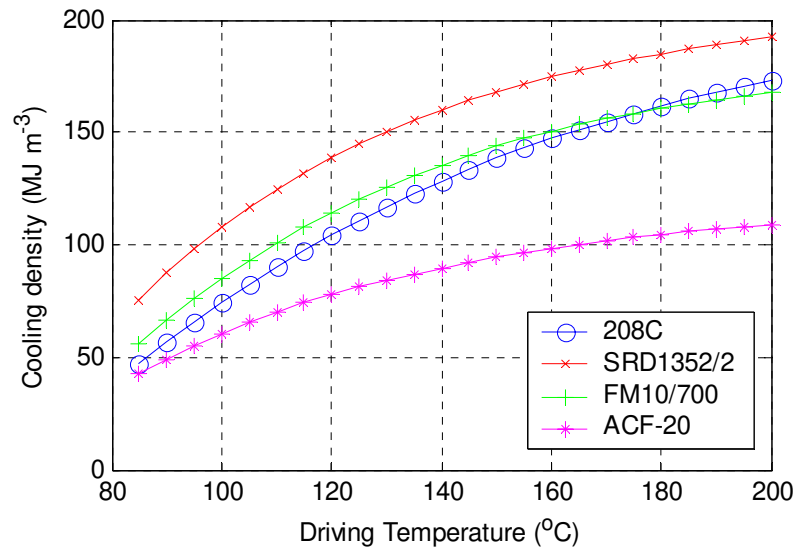
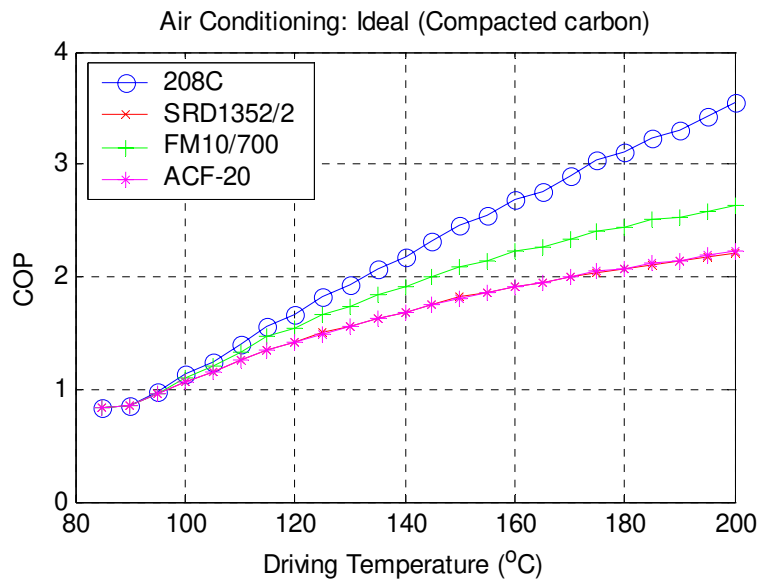
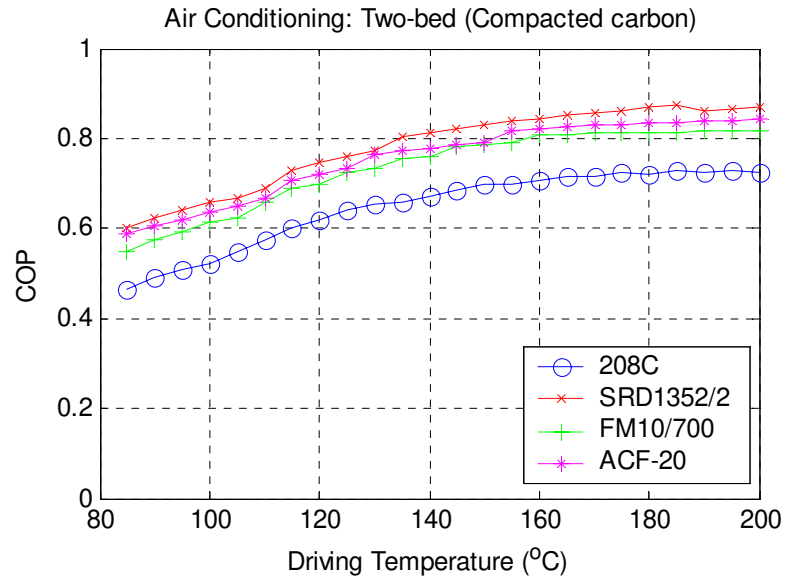
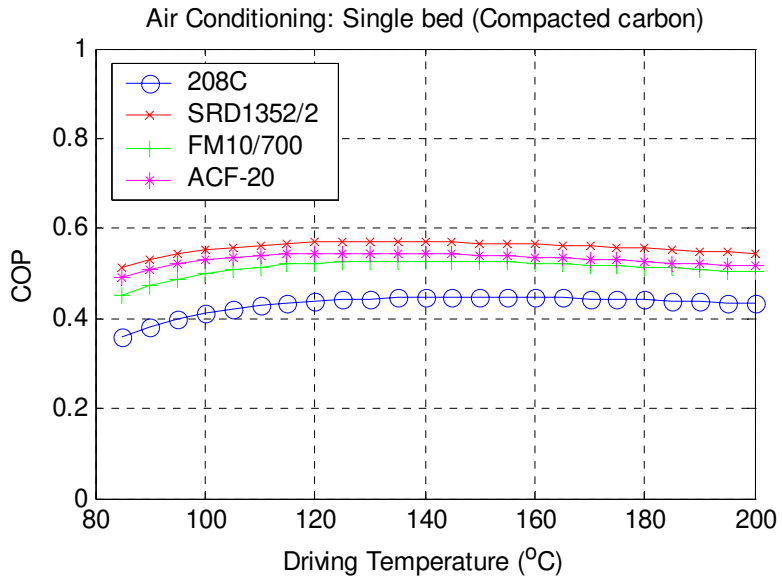


Figure 15: Air conditioning using carbon compacted

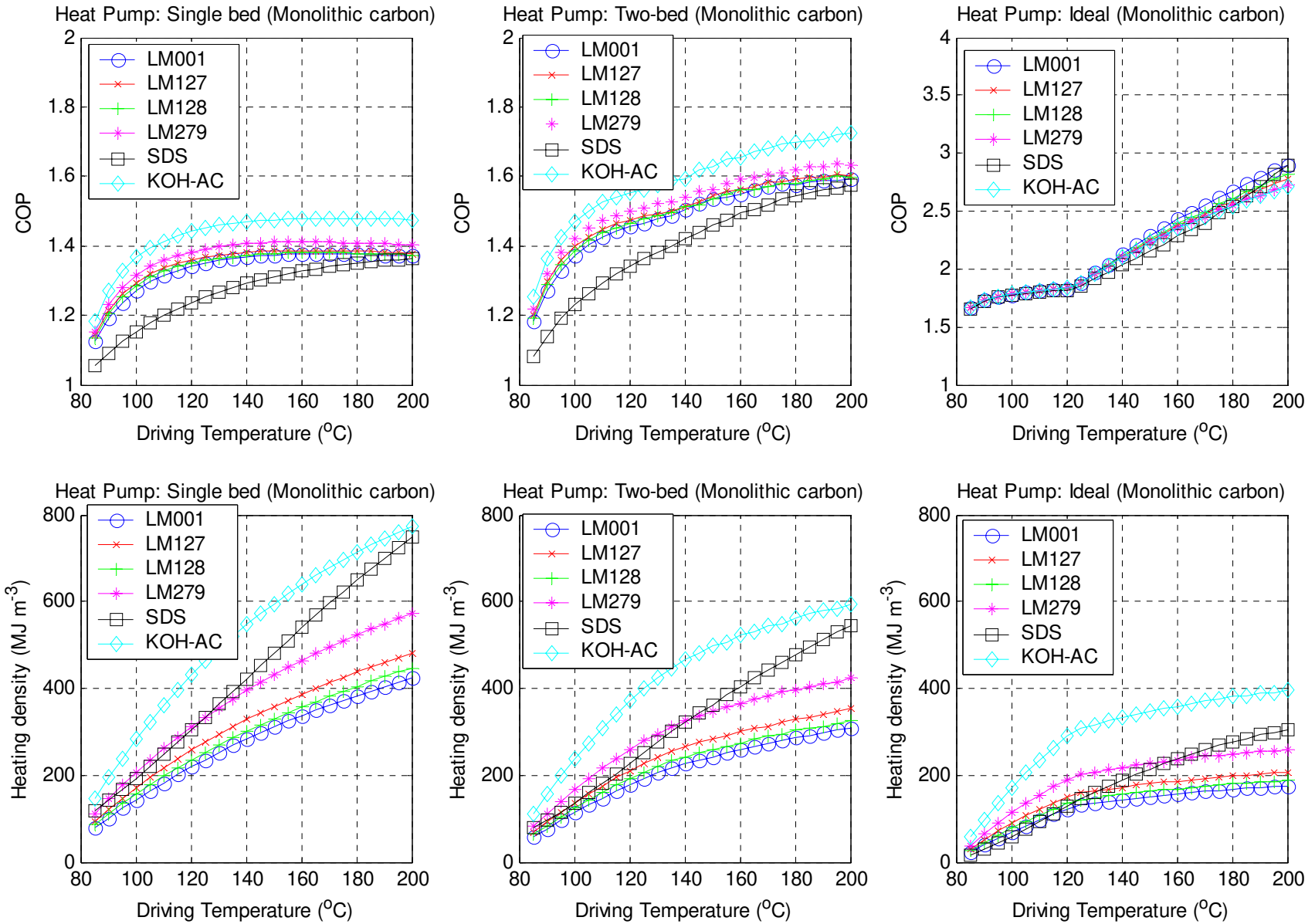


Figure 16: Heat pump using monolithic carbon

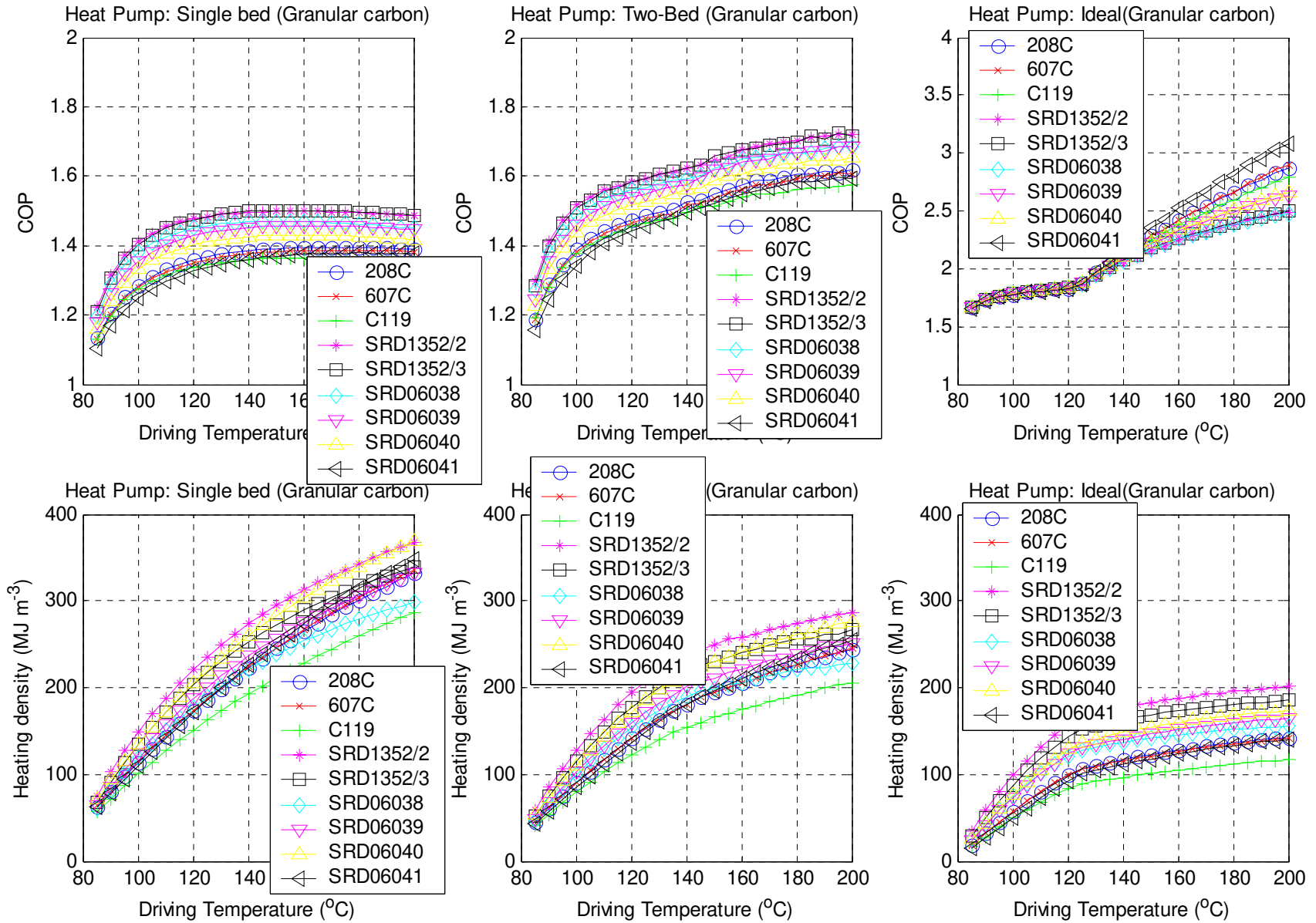


Figure 17: Heat pump using granular carbon

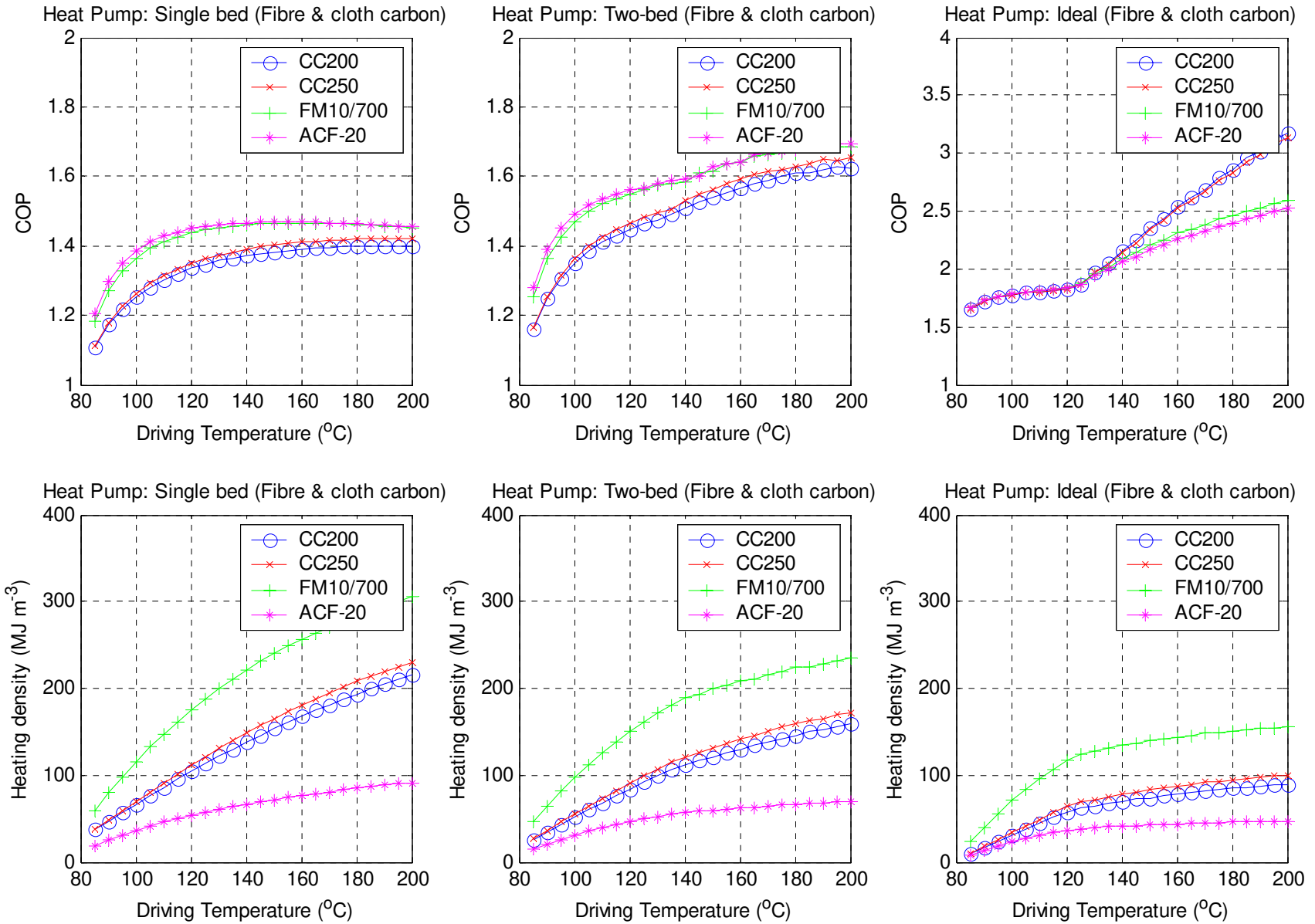


Figure 18: Heat pump using carbon fibre and cloth

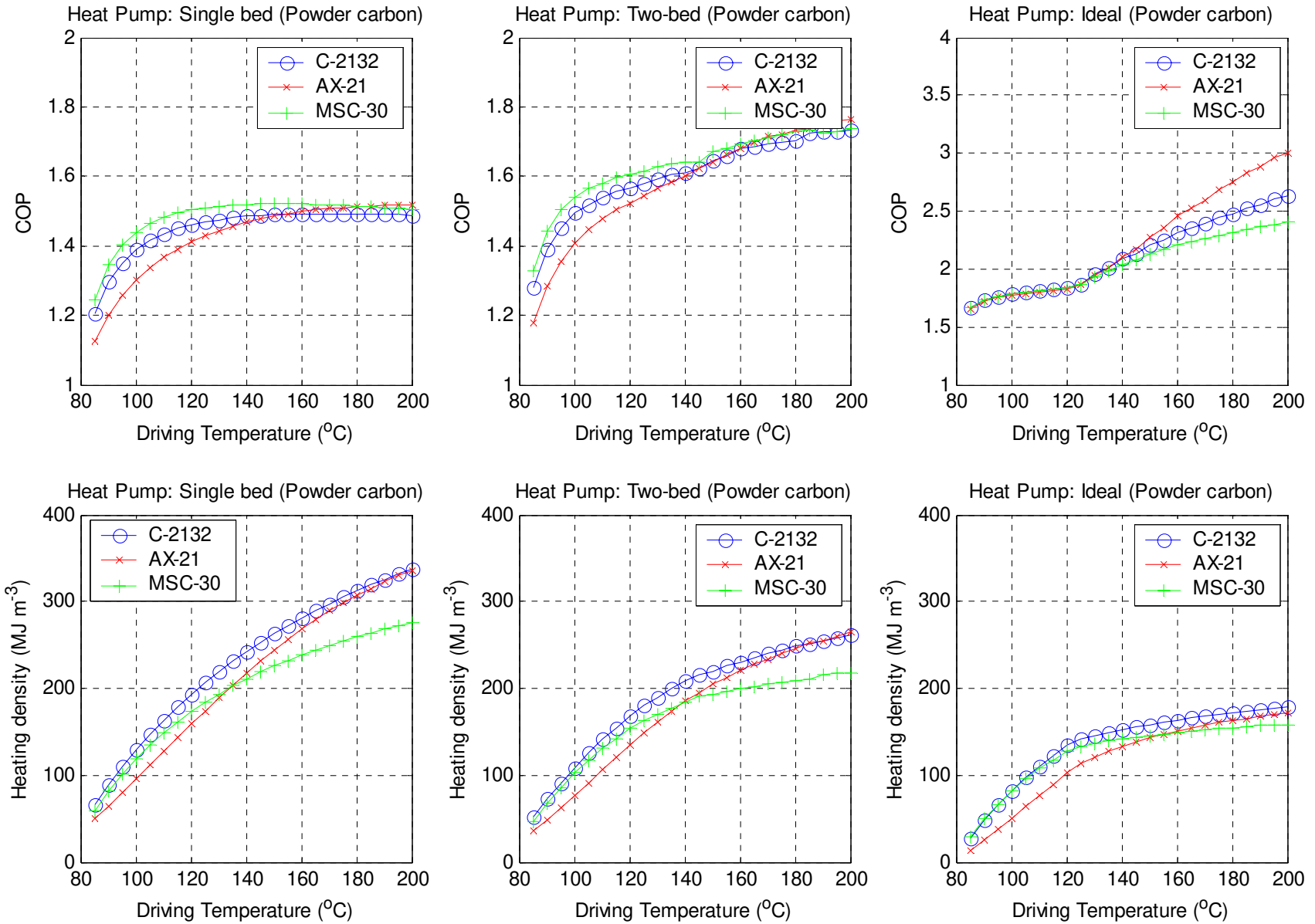


Figure 19: Heat pump using carbon powder

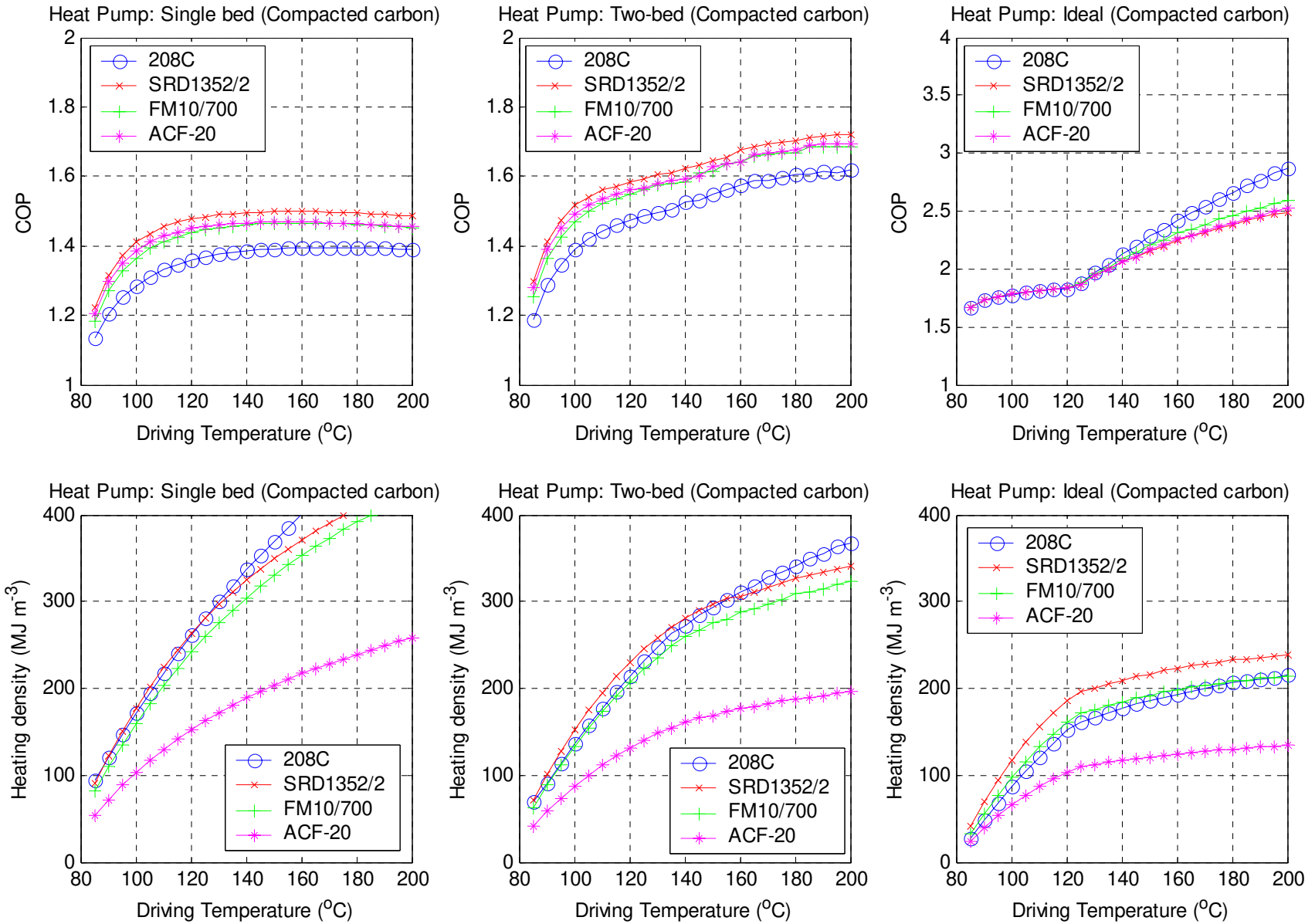


Figure 20: Heat pump using compacted carbon

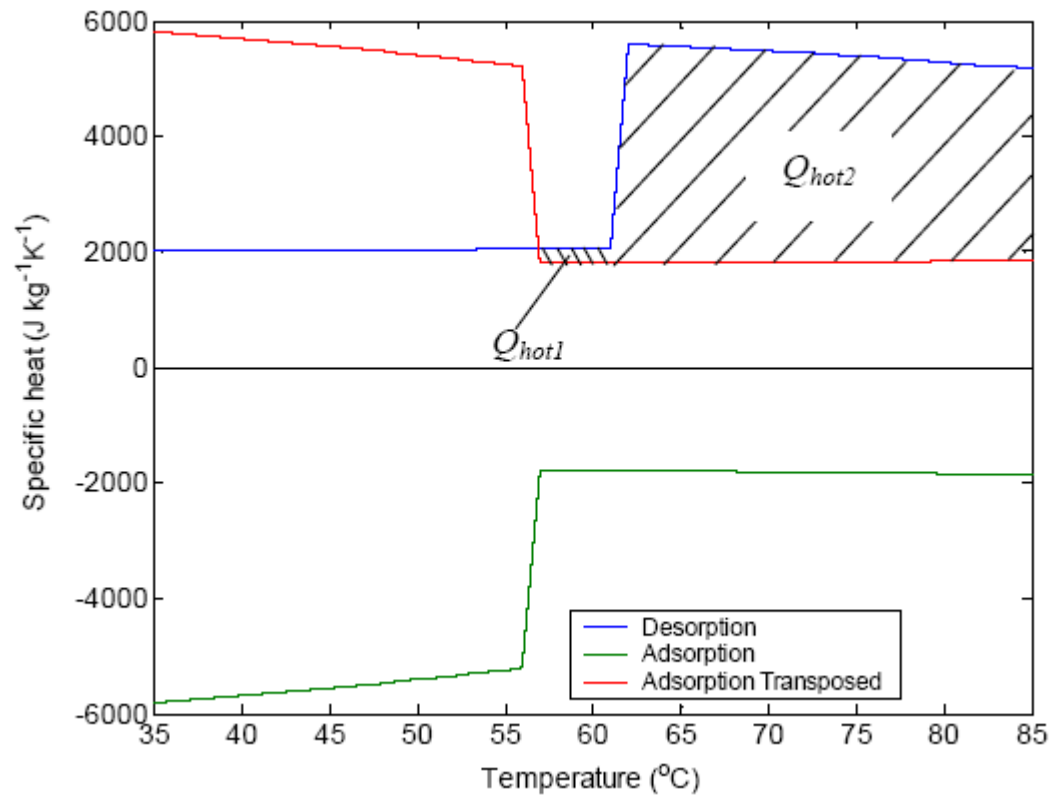


Figure 21: Bed specific heat capacity for 208C in the air conditioning application with a driving temperature of 85°C

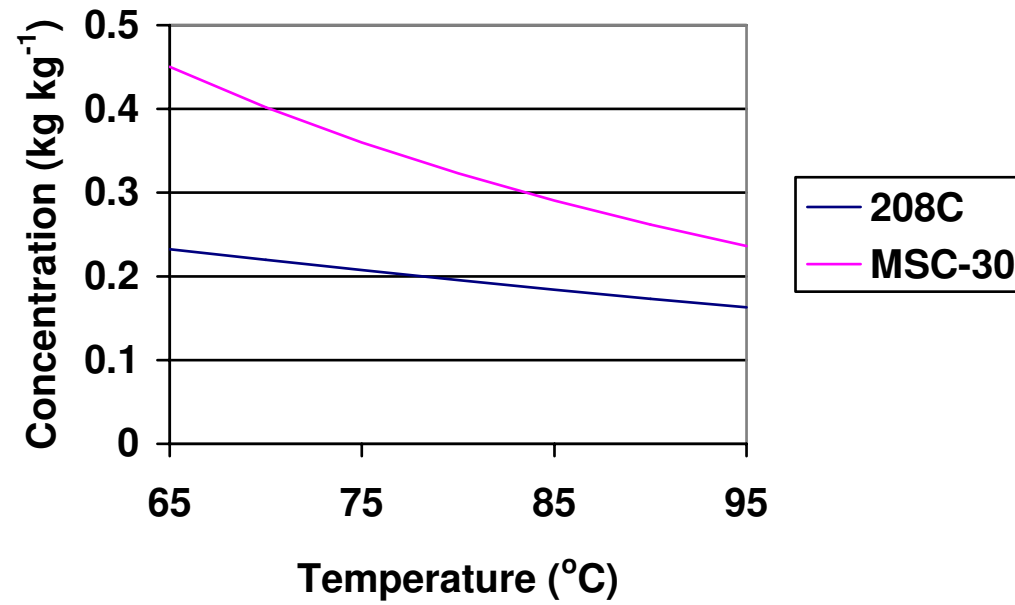


Figure 22: Temperature-concentration for two carbons during desorption in the air conditioning application at low driving temperature

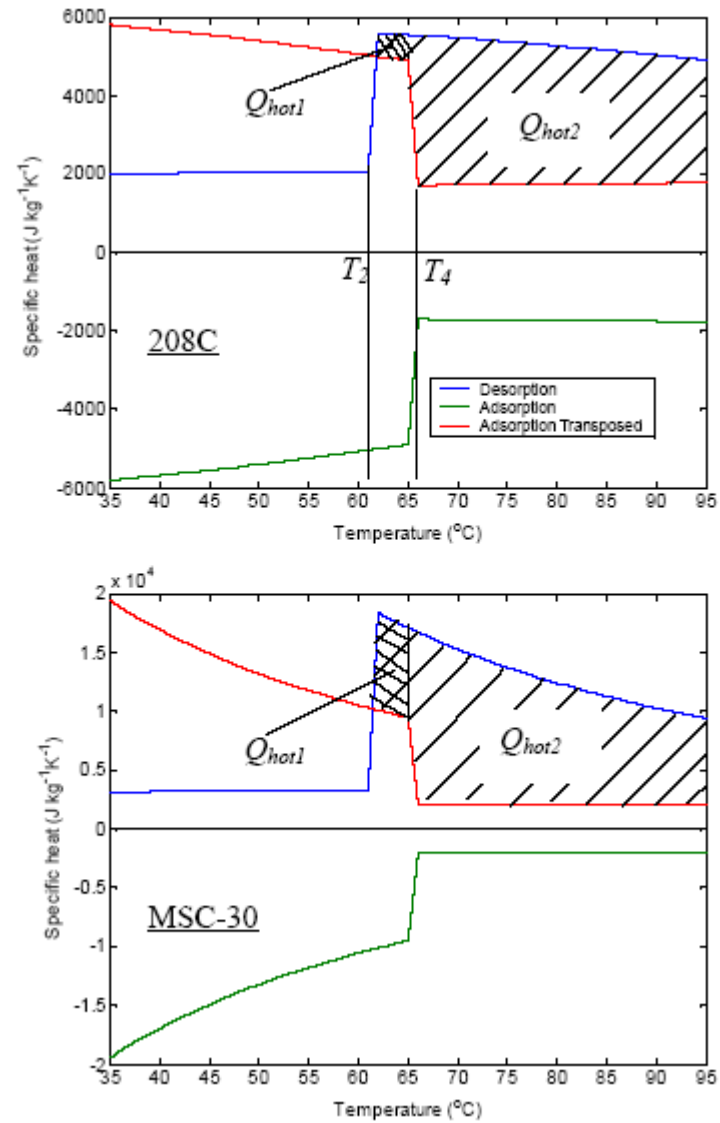


Figure 23: Bed heat capacity for adsorption and desorption for 208C and MSC-30 in the air conditioning application with a driving temperature of 95°C.

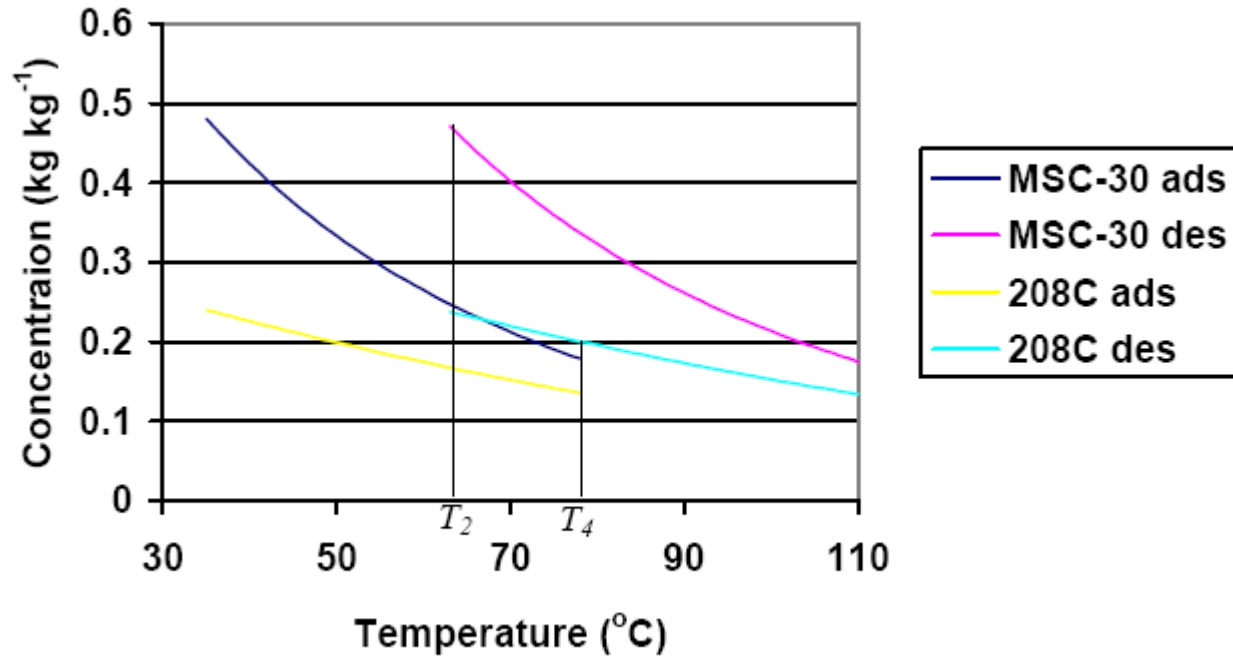


Figure 24: Concentration profiles during adsorption and desorption for 208C and MSC-30 for the air conditioning application with a driving temperature of 110°C.